

Atmospheric oxidation of 1,3-butadiene: characterization of gas and aerosol reaction products and implication for PM_{2.5}

M. Jaoui¹, M. Lewandowski², K. Docherty¹, J. H. Offenberg², and T. E. Kleindienst²

¹Alion Science and Technology, P.O. Box 12313, Research Triangle Park, NC 27709, USA

²US Environmental Protection Agency, Office of Research and Development, National Exposure Research Laboratory, Research Triangle Park, NC 27711, USA

Correspondence to: M. Jaoui (jaoui.mohammed@epa.gov); phone: (919) 541-7728

Abstract

Secondary organic aerosol (SOA) was generated by irradiating 1,3-butadiene (13BD) in the presence of H_2O_2 or NO_x . Experiments were conducted in a smog chamber operated in either flow or batch mode. A filter/denuder sampling system was used for simultaneously collecting gas- and particle-phase products. The chemical composition of the gas phase and SOA was analyzed using derivative-based methods (BSTFA, BSTFA + PFBHA, or DNPH) followed by gas chromatography–mass spectrometry (GC-MS) or high-performance liquid chromatography (HPLC) analysis of the derivative compounds. The analysis showed the occurrence of more than 60 oxygenated organic compounds in the gas and particle phases, of which 31 organic monomers were tentatively identified. The major identified products include glyceric acid, *d*-threitol, erythritol, *d*-threonic acid, *meso*-threonic acid, erythrose, malic acid, tartaric acid, and carbonyls including glycolaldehyde, glyoxal, acrolein, malonaldehyde, glyceraldehyde, and peroxyacryloyl nitrate (APAN). Some of these were detected in ambient $\text{PM}_{2.5}$ samples and could potentially serve as organic markers of 1,3-butadiene (13BD). Furthermore, a series of oligoesters were detected and found to be produced through chemical reactions occurring in the aerosol phase between compounds bearing alcoholic groups and compounds bearing acidic groups. Time profiles are provided for selected compounds. Time profiles are provided for selected compounds.

SOA was analyzed for organic mass to organic carbon (OM/OC) ratio, effective enthalpy of vaporization ($\Delta H_{\text{vap}}^{\text{eff}}$), and aerosol yield. The average OM/OC ratio and SOA density were 2.7 ± 0.09 and 1.2 ± 0.05 , respectively. The average $\Delta H_{\text{vap}}^{\text{eff}}$ was $26.1 \pm 1.5 \text{ kJ mol}^{-1}$, a value lower than that of isoprene SOA. The average laboratory SOA yield measured in this study at aerosol mass concentrations between 22.5 and $140.2 \mu\text{g m}^{-3}$ was 0.025 ± 0.011 , a value consistent with the literature (0.021–0.178). While the focus of this study has been examination of the particle-phase measurements, the gas-phase photooxidation products have also been examined.

The contribution of SOA products from 13BD oxidation to ambient $\text{PM}_{2.5}$ was investigated by analyzing a series of ambient $\text{PM}_{2.5}$ samples collected in several locations around the United States. In addition to the occurrence of several organic compounds in field and laboratory samples, glyceric acid, *d*-threitol, erythritol, erythrose, and threonic acid were found to originate only from the oxidation of 13BD based on our previous experiments involving chamber oxidation of a series of hydrocarbons. Initial attempts have been made to quantify the

concentrations of these compounds. The average concentrations of these compounds in ambient
PM_{2.5} samples from the California Research at the Nexus of Air Quality and Climate Change
(CalNex) study ranged from 0 to approximately 14.1 ng m⁻³. The occurrence of several other
compounds in both laboratory and field samples suggests that SOA originating from 13BD
oxidation could contribute to the ambient aerosol mainly in areas with high 13BD emission rates.

Keywords: 1,3-butadiene, erythrose, threitol, erythritol, glyceric acid, threonic acid, SOA

1 **Introduction**

2 Atmospheric organic carbon (OC) from anthropogenic sources forms a large portion of
urban ambient organic aerosol. During the last century, the source of anthropogenic hydrocarbons
4 increased significantly due to growth in population and energy demand. The sources of these
hydrocarbons are as varied as the species that make up the organic aerosol, and their oxidation is
6 known to lead to the formation of organic aerosol. In the last two decades, considerable effort has
been devoted to understanding secondary organic aerosol (SOA) and ground-level ozone
8 formation from biogenic and anthropogenic hydrocarbons (Kanakidou et al., 2005; Hallquist et al.
2009). SOA often constitutes a significant fraction of particles less than 2.5 micrometers in
10 diameter (PM_{2.5}) and can have significant impacts on the physical and chemical characteristics of
ambient aerosol affecting climate and air quality from global to regional and local scales.
12 Numerous studies have shown that several atmospheric processes including visibility reduction
(Sisler and Malm, 1994) and changes in direct radiative forcing that might affect the global
14 climate (Charlson et al., 1992) are affected by ambient PM_{2.5}. Exposure to PM_{2.5} has been
implicated in increases in human mortality and morbidity levels, and decreased PM levels have
16 been shown to be associated with increased life expectancy (Pope et al., 2009). To date, the
chemical composition of ambient aerosol particles, in particular the organic fraction originating
18 from anthropogenic sources, has not been fully characterized. As the understanding of the
chemical composition and toxicology associated with these particles develops, more accurate
20 compositional data might be required.

 In the past, hydrocarbons possessing five or fewer carbon atoms were generally not
22 considered significant contributors to SOA formation (Grosjean and Seinfeld, 1989). Recently,
however, a series of biogenic and anthropogenic conjugated dienes with five or fewer carbon
24 atoms (e.g., isoprene, 1,3-butadiene [13BD], 2-methyl-3-butene-2-ol) have been shown to
contribute to SOA formation (Claeys et al., 2004; Edney et al., 2005; Kroll et al., 2006; Surratt et
26 al., 2006, 2010; Sato et al., 2011; Jaoui et al., 2012; Zhang et al., 2012, 2014, Angove et al.,
2006). Although significant advances have been made toward elucidating 13BD oxidation
28 products and their role in SOA formation, the importance of 13BD to atmospheric SOA formation
is not well known at present, but its contribution could be significant in urban areas influenced by
30 high 13BD emissions.

1,3-Butadiene, a conjugated diene, is considered a significant anthropogenic organic compound with an annual emission rate of 6 million tons worldwide (Berndt and Böge, 2007), and can serve as a functional analog for isoprene. 13BD is widely used in the chemical industry mainly through processing of petroleum to make synthetic rubber, resins, and plastics (Berndt and Böge, 2007). 13BD is classified as a hazardous compound in the 1990 Clean Air Act Amendments (CAAA; US EPA, 1996), a carcinogenic and toxic pollutant, and a genotoxic chemical in humans and other mammals (Acquavella, 1996; US EPA, 2002). The main sources of 13BD in the atmosphere include automobile exhaust as a combustion byproduct, tobacco smoke, gasoline evaporative emissions, biomass burning, and forest fires (Anttinen-Klemetti et al., 2006; Dollard et al., 2001; Eatough et al., 1990; Pankow et al., 2004; Penn and Snyder, 1996; Ye et al., 1998; Thornton-Manning et al., 1997; Sorsa et al., 1996; Hurst, 2007). The mixing ratio of 13BD at the low ppb level was measured in the ambient atmosphere (US EPA, 2002; Dollard et al., 2001; Vimal et al., 2008; Duffy and Nelson, 1997), while higher concentrations up to 15 ppb have been observed in areas close to plastic and rubber facilities, inside moving vehicles, and in road traffic tunnels. Due to the relatively high volatility of 13BD, its main removal from the atmosphere is through reactions with OH, O₃, NO₃, and Cl to produce a number of potentially toxic products (e.g., acrolein, formaldehyde), which are also considered air toxics under the CAAA (Liu et al., 1999; Notario et al., 1997; Kramp and Paulson, 2000; Doyle et al., 2004; Angove et al., 2006).

The gas-phase oxidation of 13BD has been investigated in a series of laboratory studies. Most work to date has involved the use of flow tubes and smog chambers to study gas-phase kinetics of 13BD, but in only a few cases have aerosol products been examined. Liu et al. (1999) examined the gas-phase products from the reaction of 13BD with OH radicals and ozone (O₃). The major carbonyl products reported were formaldehyde, acrolein, glycolaldehyde, glyceraldehyde, 3-hydroxy-propanaldehyde, hydroxyacetone, and malonaldehyde. Additional non-carbonyl products included furan, 1,3-butadiene monoxide, and 1,3-butadiene diepoxide. Berndt and Böge (2007) reported yields of formaldehyde (0.64 ± 0.08), acrolein (0.98 ± 0.12), 4-hydroxy-2-butanal (0.23 ± 0.10), nitrates (0.06 ± 0.02), and furan (0.046 ± 0.014) from the OH radical reactions with 13BD conducted in a flow reactor. Kramp and Paulson (2000) studied the formation of two toxic gas reaction products, acrolein and 1,2-epoxy-3-butene, from the ozonolysis of 13BD and reported yields of $52 \pm 7\%$ for acrolein and $3.1 \pm 0.5\%$ for 1,2-epoxy-3-

butene. Sato (2008) reported the presence of nitric acid, glyoxylic acid, pyruvic acid, oxalic acid, tetrols, nitrooxybutanetriols, and dinitrooxybutanediols in an experiment involving the photooxidation of 13BD/NO/CH₃ONO/air mixture in which an SOA yield of 0.025 was found. Recently, Sato et al. (2011) studied SOA formation from 13BD/NO_x and 13BD/NO_x/H₂O₂ reactions and found SOA yields between 0.021 and 0.178. In that study, a series of oligomeric compounds were tentatively identified including glyceric acid oligomers and oligoesters formed from the dehydration reaction of nitrooxypolyols and glyceric acid. To date, there have been very limited studies on SOA characterization, and only a few reaction products have been reported (Sato et al., 2011).

The detection of glyceric acid, glycerol, threitol, and erythritol in forest and tropical ambient samples (Decesari et al., 2006; Wang et al., 2008; Claeys et al., 2010; Fu et al., 2010), in which erythritol was considered a marker for fungal spores or biomass burning (Claeys et al., 2010; Fu et al., 2010), clearly suggests the importance of 13BD chemistry in the atmosphere. Laboratory experiments have shown that glyceric acid, which has a skeleton with four carbon atoms similar to that of 13BD, represents a building block of oligomers and oligoesters in 13BD SOA (Sato et al., 2011). High emissions of 13BD in urban areas could be a significant source of C₄ polyols, ozone, acrolein, and formaldehyde and could influence the urban atmospheric chemistry. C₄ polyols, which are known to have high water solubility, were not found to contribute to cloud formation any more than other atmospheric organic compounds (Ekström et al., 2009).

Given the presence of threitol, erythritol, and glyceric acid in forest areas and the high emission of 13BD (a possible precursor to these compounds) in rural areas, it is crucial to assess the extent to which we understand SOA formation from the oxidation of 13BD. In this paper, gas and particle organic compounds from the photooxidation of 13BD in the presence and absence of NO_x were examined. Reaction products in the gas-phase were measured using derivatization and non-derivatization techniques. Organic compounds in the particle phase were examined as well as aerosol yields and other aerosol properties. The main focus was to identify organic compounds that can be used as possible unique markers in ambient aerosol. Based on the analysis of field and laboratory samples, the tracer method reported by Kleindienst et al., 2007 was then used to estimate the contribution of 13BD to organic aerosol in ambient air.

2 Materials and methods

2 All chemicals, including the derivatization reagents *O*-(2,3,4,5,6-
pentafluorobenzyl)hydroxylamine hydrochloride (PFBHA) and a combination of *N,O*-
4 *bis*(trimethylsilyl) trifluoroacetamide (BSTFA) with 1% of trimethylchlorosilane (TMCS) as
catalyst, were purchased from Aldrich Chemical Co. (Milwaukee, WI) at the highest purity
6 available and were used without further purification.

Experiments were conducted in a 14.5 m³ parallel-piped, stainless-steel, fixed-volume
8 chamber with 40- μ m TFE Teflon coated walls. A combination of fluorescent bulbs was used in
the chamber to provide radiation distributed over the actinic portion of the spectrum similar to
10 solar radiation between 300 and 400 nm. UV-313 sunlamps were also used for some irradiations
in the absence of NO_x. The smog chamber was operated either in static mode (as a conventional
12 batch reactor) or for experiments requiring large sampling volumes in dynamic mode (flow mode)
to produce a steady-state concentration of gas-and particle-phase reaction products. The relative
14 humidity and temperature were measured using an Omega Engineering, Inc. (Stamford, CT)
digital thermo-hygrometer (model RH411). An integrating radiometer (Eppley Laboratory, Inc.,
16 Newport, RI) was used to monitor light intensity continuously. Details of the chamber and its
operation can be found in Kleindienst et al. (2006).

18 Experiments were conducted in either the absence or presence of NO_x. The influence of
aerosol acidity as well as relative humidity on SOA formation is described in an accompanying
20 paper (Lewandowski et al., 2014). For experiments with NO_x, 13BD and NO were added to the
chamber through flow controllers to the target concentration. For experiments in the absence of
22 NO_x, the photolysis of H₂O₂ was the source of OH. H₂O₂ as a 50% aqueous solution was injected
through a syringe pump into a heated glass bulb where it vaporized and then was mixed rapidly
24 by the main dilution air flow. H₂O₂ concentrations were determined by UV absorption using a
conventional ozone monitor, as described previously (Kleindienst et al., 2009). For these
26 experiments, 13BD was added as described above. Ammonium sulfate seed aerosol was also
introduced into the chamber for all experiments to serve as a condensing medium for semivolatile
28 organic products that might form.

NO and NO_x were monitored with a TECO (Franklin, MA) oxides of nitrogen analyzer
30 (model 42C) with an in-line nylon filter used to prevent nitric acid from entering the analyzer.

Ozone was measured with a Bendix (Lewisburg, WV) ozone monitor (model 8002). 13BD concentrations were measured in the inlet and within the chamber in a semi-continuous fashion by gas chromatography with flame ionization detection (GC-FID).

Low molecular weight carbonyl and dicarbonyl compounds including formaldehyde, glyoxal, and acrolein were identified and quantified using derivatization with DNPH (2,4-dinitrophenyl-hydrazine). Air samples were drawn during 20 min at a rate of 0.50 l min⁻¹ through an impinger containing 5 ml of a DNPH solution in acetonitrile. The resulting solutions were analyzed by high-performance liquid chromatography with ultraviolet detector (HPLC/UV) (Smith et al., 1989). An external standard solution containing 16 hydrazones and dihydrazones was used for the identification and quantification of compounds formed during the reaction. For carbonyl compounds that standards are not available, the technique allows their concentrations to be estimated from the average molar extinction coefficient of the standard compounds. Since the extinction coefficient is largely dependent on the chromophore and not the substituent group (Smith et al., 1989), these hydrazones show a high degree of consistency. Peroxyacryloyl nitrate (APAN) was also measured in this study.

Gas-phase compounds with higher molecular weights were collected with 60-cm, four-channel XAD4-coated annular denuders. The denuders were analyzed for organic compounds by extracting them in a 1:1 dichloromethane/methanol mixture and then derivatizing with a BSTFA/TMCS mixture (Jaoui et al., 2004). Ketopinic acid (KPA) was used as an internal standard. Extracts were then analyzed by gas chromatography–mass spectrometry (GC-MS) using the techniques described below.

Organic carbon concentrations in the particles were measured using a semi-continuous elemental carbon–organic carbon (EC-OC) instrument (Sunset Laboratories, Tigard, OR). The OC-EC instrument uses a quartz filter housed within the oven for the analysis. SOA from the chamber was pumped at a rate of 8 l min⁻¹ through the quartz filter. To remove the interference of gas-phase organic compounds in the effluent, a carbon-strip denuder was placed in-line before the quartz filter. The duty cycle for the OC measurement was 0.75 h, with a sample collection time of 0.5 h and an analysis time of 0.25 h.

A SMPS (Scanning Mobility Particle Sizer) (model 3071A, TSI, Inc., Shoreview, MN) and a CPC (Condensation Particle Counter) (model 3010, TSI, Inc., Shoreview, MN) instruments

were used to measure the aerosol size distribution, volume, and total number density. The SMPS operating conditions were 2 L min⁻¹ sheath flow, 0.2 L min⁻¹ sample flow, and 19 to 982 nm size scan. The effective enthalpies of vaporization of 13BD aerosol were measured also with the SMPS by adding a heated inlet, which allows the aerosol to be subjected to a range of fixed temperatures (Offenberg et al., 2006).

Aerosol samples were collected at a flow rate of 15 l min⁻¹ with 47-mm glass-fiber filters (Pall Gelman Laboratory, Ann Arbor, MI) for off-line analysis. These samples were sonicated with methanol, and the extracts were derivatized with a BSTFA/TMCS mixture (Jaoui et al., 2004). The resulting derivatized extracts were analyzed by GC-MS on a ThermoQuest (Austin, TX) GC coupled with an ion trap mass spectrometer. The temperature of the injector was 270 °C, and was operated in splitless mode. A 60-m, 0.25-mm inner diameter, RTx-5MS column (Restek, Inc., Bellefonte, PA) with a 0.25-μm film thickness was used. The oven initial temperature was 84 °C for 1 min, then increased by a temperature ramp of 8 °C min⁻¹ to 200 °C, followed by a 2-min hold, and then a second ramp of 10 °C min⁻¹ to 300 °C. The ion source, ion trap, and interface temperatures were 200, 200, and 300 °C, respectively. 2 ul of the extract was injected in CI and/or EI modes.

For the batch mode experiments, NO_x and 13BD were introduced continuously into the chamber at the beginning of the experiment until steady state was reached. Then the reaction was started by turning off the reactant (NO_x and 13BD) flows at the same time the lights were turned on. Samples were taken for gas and particle constituents at sampling periods appropriate for the required masses needed for analysis. In flow mode experiments, reactants were added to the chamber continuously and the effluent was withdrawn at the same flow rate for filter collection and on-line gas and particle analysis. The chamber was operated as a batch reactor in experiments ER439 and ER442 and as a flow reactor with a nominal total flow of 60 l min⁻¹ to produce the steady-state reaction mixtures in ER440, ER441, ER443, and ER444 (Table 1). Irradiation ER439 was conducted as a survey experiment only and was used in GC-MS analysis to identify compounds. Experiment ER442, in which six sample denuders and filters were collected simultaneously, was carried out to investigate time profiles of reaction products using a BSTFA/TMCS mixture derivatization. The dynamic experiments were also conducted in stages by irradiating 13BD/NO_x or 13BD/H₂O₂ mixtures in the absence or presence of SO₂ or acidic seed to produce acidic sulfate aerosol. For these experiments, the reactant mixture at each stage

was allowed to come to steady state over a period of 18 to 24 h before sampling began. The results of these experiments are reported in an accompanying paper (Lewandowski et al., 2014).

In addition to laboratory experiments, ambient PM_{2.5} samples were collected on either quartz or Teflon-impregnated glass-fiber filters. Field sample filters were Soxhlet extracted, and the resulting extracts were evaporated to dryness and derivatized with a BSTFA/TMCS mixture (Jaoui et al., 2004). Detailed descriptions of some of these field campaigns have been provided by Lewandowski et al. (2007, 2008) and Kleindienst et al. (2010). The focus of the field sample analysis has been to investigate the presence of 13BD organic tracer compounds in ambient PM_{2.5}.

3 Results and discussion

The initial conditions for experiments involving the oxidation of 13BD are given in Table 1. For experiments conducted in the presence of NO_x, the initial 13BD concentrations ranged from 3.2 to 8.4 ppmC and the NO concentrations ranged from 340 to 917 ppb. Most experiments were conducted under dry conditions (RH < 3%) except for ER444-1 (Table 1). In the absence of NO_x, initial H₂O₂ concentration was 2.2 ppm for ER441-1) and 3.8 ppm for ER443-1.

ER439 was conducted as a survey experiment in which sufficient aerosol mass was collected on glass-fiber (GF) filters and used for GC-MS analysis solely for the purpose of identifying reaction products. The gas-phase and aerosol extracts were solvent extracted, derivatized, and analyzed by GC-MS or HPLC. Gas and aerosol extracts were derivatized using BSTFA or PFBHA + BSTFA double derivatization. These techniques provide a sensitive method for identifying and quantifying low concentrations of lightly to highly oxidized organic compounds. The BSTFA single derivatization technique provides good quantitative analysis due to both its simplicity and its efficiency (Jaoui et al., 2004). Although the double derivatizations are not quantitatively rigorous, they provide additional structural information that aids in identification of organic constituents by derivatizing the carbonyls that otherwise would not be detected by BSTFA derivatization alone.

The analysis of laboratory-generated gas-phase and SOA products from 13BD oxidation shows a series of organic compounds containing ketone, carboxylic acid, and/or alcoholic

functions. Many of these compounds do not have authentic standards and their identifications were based on the interpretation of the mass spectra of the derivatized compound (Jaoui et al., 2004, 2005). The identification should be regarded as tentative except for compounds that have authentic standards. The recognition of characteristic ions associated with a particular derivatization scheme was used to guide the analysis of chemical ionization (CI) mass spectra of the derivatives. BSTFA reacts with -COOH and -OH groups to form BSTFA derivatives. Characteristic ions are m/z 73, 75, 147, and 149. Adduct ions from the derivatives include m/z $M^+ + 73$, $M^+ + 41$, $M^+ + 29$, and $M^+ + 1$; fragment ions include m/z $M^+ - 15$, $M^+ - 73$, $M^+ - 89$, $M^+ - 117$, $M^+ - 105$, $M^+ - 133$, and/or $M^+ - 207$. PFBHA reacts with each nonacidic $>C=O$ group to form an oxime derivative. In CI mode, the base peak for most oximes is $M^+ + 1$ or 181, while other fragments/adducts include m/z $M^+ + 29$, $M^+ + 41$, $M^+ - 181$, and $M^+ - 197$. Double derivatizations result in adducts and fragments that include characteristic ions from each single derivatization. In many cases, samples were run in electron ionization (EI) mode to produce greater fragmentation for additional structural information.

3.1 Product identification

In the present study, mass spectra of more than 60 derivative compounds have been recorded for which representative examples are shown. The approach used for their identification is as follows: Peaks detected in blank and background chamber samples were eliminated first. A peak was associated with a reaction product only if its corresponding mass spectrum was consistent with the fragmentation pattern of the derivatization reagent used as noted above. All recorded spectra were compared with spectra derived from various reference compounds and the literature. Typical total ion chromatograms of samples taken from experiment ER439 (Table 1) are shown in Figure 1 as BSTFA (top) and PFBHA + BSTFA (bottom) derivatives of 13BD SOA. For clarity, only the main products are shown. GC-MS analysis of the mixture showed the presence of 10 significant peaks in the BSTFA derivatives and seven significant peaks in the PFBHA + BSTFA derivatives. However, a significant number of relatively small peaks associated with both derivatizations were clearly observed in the particle phase, reflecting the complexity of the oxidation of 13BD. Compounds identified in the present study are summarized

in Table 2, which contains proposed structures for products identified when possible as well as molecular weights (MWs) of the underivatized compounds (Mc).

3.1.1 SOA products

Aerosol parameters. The production of aerosol was found to be dependent on the conditions under which the experiments were carried out, in particular the presence of NO_x in the system. The oxidation of 13BD produced non-negligible levels of aerosol. Except for a minor organic nitrate channel, the photooxidation system in the presence of NO_x converts virtually all RO₂ formed into RO radicals, which then decompose or isomerize to produce carbonyl or hydroxycarbonyl compounds (Atkinson, 2000). Without NO_x in the system, RO₂ radicals typically react with HO₂ or self-react to produce a product molecule with four carbons while adding functional groups to the product. These products are sufficiently nonvolatile to condense into the particle phase.

The secondary organic carbon yield (Y_{SOC}) and secondary organic aerosol yield (Y_{SOA}) are generally defined using the following relationships: $Y_{SOC} = SOC/\Delta HC_C$ and $Y_{SOA} = SOA/\Delta HC$, where SOC is the corrected organic carbon concentration, ΔHC is the reacted hydrocarbon mass concentration, and ΔHC_C is the reacted carbon mass concentration of the hydrocarbon obtained from Table 3. The SOA concentration was obtained from gravimetric measurement. The volume concentrations from the SMPS (nl m⁻³) are also reported in Table 3. The SOA density was estimated using both filter masses and SMPS data (Table 4). An average density of 1.2 ± 0.05 was obtained. Organic carbon and organic aerosol yields and organic mass to organic carbon ratio (OM/OC) were determined for experiments in which the chamber was operated in a dynamic mode (Table 4). Uncertainties in the yields come from the experimental uncertainties in SOA and the reacted 13BD concentrations. The gravimetric yield values were similar to those measured using the SMPS data. Average SOA and SOC yields of 0.025 ± 0.011 and 0.017 ± 0.013 were obtained, respectively. SOA yield values were in reasonable agreement with data in the literature (Sato et al., 2011; Sato, 2008). In addition, the effective enthalpy of vaporization (ΔH_{vap}^{eff}) was measured for the different experiments conducted in this study, and its average value was found to be 26.1 ± 1.5 kJ mol⁻¹.

Characterization of SOA products. SOA generated from 13BD oxidation was dominated by

oxygenated compounds in which 13BD double bonds were oxidized. Chromatograms from SOA samples either in EI or CI modes indicated the presence of several larger peaks from either BSTFA or PFBHA + BSTFA derivatizations. Figure 2 shows examples of CI mass spectra as BSTFA derivatives for some products detected and identified in the aerosol phase.

A glyceric acid (GA or 2,3-dihydroxypropanoic acid) peak eluted at 18.92 min was one of the largest peaks detected in the chromatogram in Figure 1 (top). The GA mass spectrum (Figure 2, bottom left) shows strong characteristic fragments ions at m/z 323 ($M^+ + 1$), 189 ($M^+ - 133$), 205 ($M^+ - 117$), and 307 ($M^+ - 15$) and adducts at $M^+ + 1$, $M^+ + 29$, and $M^+ + 41$ that are consistent with the presence of three (-OH) groups, indicating a BSTFA derivatized molecular weight (Md) of 322 Da (all derivatized and underivatized masses are Dalton (Da) but are not designated as such hereafter).

The BSTFA CI mass spectrum of L-threitol shows characteristic fragment ions at m/z 73, 395 [$M^+ - 15$], 321 [$M^+ - 89$], and 305 [$M^+ - 105$] and adduct at 411 [$M^+ + 1$]. These fragments and adduct are consistent with the presence of four OH groups and a MW of 410 for the derivatized compound and 122 for the underivatized compound. The presence of a peak at m/z 305 [$M^+ - 105$] is consistent with a compound bearing an alcoholic OH group. This mass spectrum is identical to the one from an L-threitol standard (Figure 2). The mass spectra of BSTFA derivatives of L- and DL-threitol standards (Figure 2, top left) are very similar (eluting at the same time) and are only slightly different from the *meso*-erythritol spectrum (Figure 2, top right); however, they elute at two different retention times. The peaks associated with these compounds, along with those of threonic acid and erythreonic acid (also called erythronic acid), are among the largest peaks observed in the chromatograms. Note that the mass spectra of the BSTFA derivative of 2-methylglyceric acid, erythrose, and 2,3-dihydroxyisopentanol (Jaoui et al., 2012) are similar, but each compound has its characteristic fragments specific to its structure (i.e., m/z 247 for erythrose, m/z 293 for 2-methylglyceric acid, and m/z 247 for 2,3-dihydroxyisopentanol). They also elute at different retention times. The mass spectrum of threonic acid (Figure 2) shows strong characteristic fragment ions at m/z 425 ($M^+ + 1$), 189 [$M^+ - 133$], 217 [$M^+ - 207$], and 409 [$M^+ - 15$] and adducts at $M^+ + 1$, $M^+ + 29$, and $M^+ + 41$. These fragmentation patterns are very similar to those observed for methyltetrols, so special caution is needed when field samples are analyzed using GC-MS to avoid designating methyltetrols as

threonic acid or erythreonic acid. Note that these compounds elute at different times and each one contains a few specific fragments (e.g., threonic acid at m/z 217, 291, and 307; methyltetrols at m/z 319 and 293).

The BSTFA CI mass spectrum of erythrose shows characteristic fragment ions at m/z 73, 321 [$M^+ - 15$], 247 [$M^+ - 89$], and 231 [$M^+ - 105$] and adducts at [$M^+ + 1$], [$M^+ + 29$], and [$M^+ + 41$]. These fragments and adducts are consistent with the presence of three OH groups and a MW of 336 for the derivatized compound and 120 for the underivatized compound. The absence of a peak at m/z 219 [$M^+ - 117$] is consistent with the absence of a carboxylic group. The mass spectrum associated with PFBHA + BSTFA double derivatization shows fragment ions at m/z 73, 181, 442 [$M^+ - 89$], and 516 [$M^+ - 15$] and adducts at [$M^+ + 1$], [$M^+ + 29$], and [$M^+ + 41$]. These fragmentation patterns are consistent with the presence of one CO group and a MW of 531 for the derivatized compound and 120 for the underivatized compound. The compound associated with these peaks was identified as erythrose (Table 2 and Figure 2). Other compounds identified in the particle phase in the present study were glyoxal, glycolaldehyde, oxalic acid, malic acid, tartaric acid, glyceraldehydes, and erythrulose (see Table 2 for more products). Additional compounds might include high molecular weight organonitrates that could have been present in the SOA or the gas phase, but were not detected by the analytical techniques used in this study (Sato et al., 2011). In addition, a large number of other smaller peaks were observed to elute late in the chromatogram in the particle phase, reflecting the complexity of the oxidation of 13BD; these were mainly associated with organoesters.

3.1.2 Oligoesters

Although several monomer compounds (e.g., glyceric acid, threitol, glycerol, erythrose, erythreonic acid, and erythritol) with MWs less than 150 were present in chamber SOA, their formation is consistent with direct oxidation of 13BD in the gas phase. A series of other smaller peaks were present in the chromatograms in which the associated mass spectra could not be associated with compounds resulting from direct gas-phase oxidation of 13BD. A detailed analysis of their mass spectra indicates high molecular weights are associated with these peaks and is consistent with oligomers or oligoesters formed through heterogeneous reactions, probably in the particle phase. Figure 3 shows 15 CI mass spectra associated with some of these peaks.

These mass spectra show characteristic fragment ions at m/z 73, $[M^+ - 15]$, $[M^+ - 89]$, $[M^+ - 117]$, and $[M^+ - 105]$ and adducts at $[M^+ + 1]$, $[M^+ + 29]$, and $[M^+ + 41]$, consistent with BSTFA derivatization for compounds bearing OH groups. Their interpretation, in general, leads to tentative structural identification since all authentic standards are unavailable.

Figure 3a, for example, shows a mass spectrum with characteristic fragment ions at m/z 73, 467 $[M^+ - 15]$, 393 $[M^+ - 89]$, 365 $[M^+ - 117]$, and 377 $[M^+ - 105]$ and adducts at 483 $[M^+ + 1]$, 511 $[M^+ + 29]$, and 523 $[M^+ + 41]$. These fragments and adducts are consistent with the presence of four OH groups and a MW of 482 for the derivatized compound and 194 for the underivatized compound. The peaks at m/z 365 $[M^+ - 117]$ and 377 $[M^+ - 105]$ are consistent with a compound bearing both a carboxylic acid group and an alcoholic OH group, respectively. The compound associated with this peak was tentatively identified as glyceric acid dimer ester (self-reaction of glyceric acid) preserving two 13BD carbon backbones connected with one oxygen atom.

Figure 3c shows a mass spectrum with characteristic fragment ions at m/z 73, 555 $[M^+ - 15]$, 481 $[M^+ - 89]$, and 465 $[M^+ - 105]$ and adducts at 571 $[M^+ + 1]$. These fragments and adducts are consistent with the presence of five OH groups and a MW of 570 for the derivatized compound and 210 for the underivatized compound. The absence of a peak at m/z 453 $[M^+ - 117]$ presents strong evidence of the absence of a carboxylic acid group, and the presence of a peak at 465 $[M^+ - 105]$ is consistent with the presence of an alcoholic OH group. The compound associated with this peak was tentatively identified as glyceric acid-tetrol ester (Table 2). Similar oligoester compounds were tentatively associated with peaks observed in chromatograms from the oxidation of 13BD (Table 2 and Figure 3). A key element for the identification of high molecular weight species resulting from 13BD oxidation is the presence or absence of peaks at m/z $[M^+ - 105]$ and/or $[M^+ - 117]$. The presence or absence of peaks at m/z $[M^+ - 105]$ and $[M^+ - 117]$ in the BSTFA mass spectrum suggests the presence or absence of alcoholic groups and carboxylic acid respectively in the compound associated with the spectrum.

The mass spectra in Figure 3 show fragmentation patterns consistent with compounds formed through esterification reactions likely occurring in the aerosol phase between an acid and an alcohol leading to the formation of an ester. This is consistent with results reported by Angove et al. (2006) and suggest the presence of C=O stretching at 1728, which is indicative of formate

esters rather than aldehydes and ketones (Angove et al., 2006). However, recent work by Birdsall et al. (2013) show that esterification reactions involving organic acid and alcohol under atmospheric conditions is too slow to occur and cannot accounts for the oligoesters observed in chamber experiments. Based on his work and prior work (Surratt et al., 2010; Lin et al., 2013), Birdsall et al. (2014) provided evidence that methacrylic acid epoxide (MAE) through hydrolysis reaction plays key role in isoprene-SOA composition.

3.2 Time profile of gas-phase and SOA products

Figure 4 (top) shows the concentrations of 13BD, O₃, NO, NO_x, and NO_x – NO; SMPS volume; and SOA as a function of irradiation time for static experiment ER442. The chamber temperature was between 19 and 22 °C during the entire experiment and the RH was < 3%. The wall loss rate constant was 0.064 h⁻¹ for SOA and SMPS. All species were corrected for dilution. SOA and O₃ remained very low at the beginning of the experiment, increased slowly as the NO was converted to NO₂, and then increased rapidly as the concentration of NO approached zero. The concentration of 13BD started with a rapid decrease that continued steadily for 2 h, after which it began to react slowly and was mostly gone by 3 h. The concentration of NO displayed a trend similar that of 13BD, while NO₂ (represented in the figure as NO_x – NO) increased at a rate similar to the decrease of NO and reached its maximum after 1 h. After NO₂ reached and maintained its maximum for approximately 1 h, it started to decrease slowly, reaching approximately 180 ppb at the end of the reaction (6 h). NO_x – NO at the end of the reaction was 176 ppb reflecting the presence of nitrated compounds, probably resulting from reaction of NO₂ with organic compounds to form organic nitrates, which are not readily analyzed using the techniques presented in this paper. Figure 4 (top) also shows that SMPS volumes and filter masses are similar. The maximum SMPS volume concentration was 130 nl m⁻³, observed at approximately 3 h when the ozone concentration reached its maximum. The profiles of the inorganic species show the characteristics of a standard volatile organic compound (VOC)/NO_x irradiation.

Of greater interest are carbonyls formed during the oxidation, shown in Figure 4 (bottom) and Table 2. The elution order of products analyzed using HPLC was established from the external hydrazone standards. Formaldehyde, acrolein, and glyoxal formed in the reaction are

clearly identified from their retention times. Note that the carbonyl products from the reaction were detected from the first DNPH sample taken at approximately 0.8 h when NO is still present in the system at relatively high concentrations. Some compounds, including glycolaldehyde, malonaldehyde, 3-hydroxypropanaldehyde, and glyceraldehyde, were identified in SOA using PFBHA + BSTFA derivatization (Figure 1, bottom, and Table 2). According to conventional reaction kinetics, OH is added to one of the double bonds in 13BD to form an RO₂ radical, which oxidizes NO to NO₂ with the resultant alkoxy radical producing a carbonyl product. Liu et al. (1999) reported the formation of several carbonyl compounds, including those observed in this study, under nighttime and/or daytime oxidation of 13BD. Several mechanistic pathways proposed by Liu et al. likely led to the formation of the major carbonyls observed in our study including glyoxal, acrolein, glyceraldehyde, and glycolaldehyde. Secondary reactions of glycolaldehyde are known to produce the dicarbonyl compound glyoxal. The importance of the dicarbonyl compounds lies in their possible significance for the formation of organic aerosol and can lead to the increased production of SOA in an aqueous or non-aqueous aerosol phase (Liu et al., 1999; Carlton et al., 2007; Liggitto et al., 2005). In our study, these compounds were detected in the aerosol phase at high levels, likely due in large part to partitioning from the gas phase.

Gas-phase and SOA components were determined quantitatively for most experiments, and data are shown here for static experiment ER442 using BSTFA derivatization. The quantification method used was similar to methods described by Jaoui et al. (2004, 2005, 2012). This quantitative analysis was based on authentic standards when available and on surrogate compounds when authentic standards could not be found commercially. Calibration factors were determined for authentic and surrogate compounds. Using our best estimates of the calibration factors, concentrations for the main compounds were determined and are provided in Figure 4 (bottom) as a function of irradiation time for compounds analyzed using the HPLC system. Figure 5 shows the time evolution of six reaction compounds—glyceric acid, erythritol, *d*-threitol, erythrose, threonic acid, and malic acid—in both gas (dashed lines) and particle (solid line) phases. All species reported in Figures 4 and 5 were analyzed using authentic standards. As can be seen in Figures 4 and 5, gas and particle compounds analyzed in this study, with the exception of glyceric acid, appear building up only when O₃ starts accumulating in the chamber. This might reflect the importance of ozone chemistry in this system. As O₃ starts accumulating in the chamber, the concentration of threonic acid and erythrose in the gas phase (Figure 4) increased

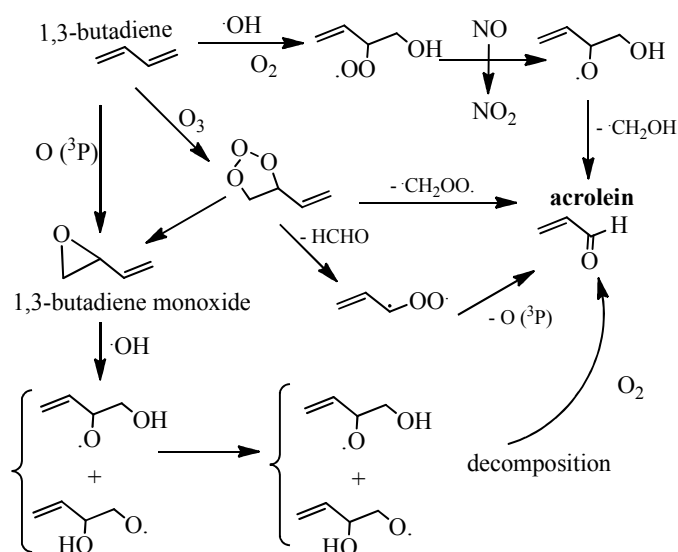
rapidly and then decreased, suggesting that secondary reactions might be occurring. These compounds were also detected in the particle phase, where their concentrations increased steadily, suggesting that partitioning of these compounds into the particle phase might also be occurring. Malic acid, *d*-threitol, and erythritol were detected only in the particle phase. Abundant compounds observed in both the gas and particle phases included glyceric acid, with maximum concentrations up to $390 \mu\text{g m}^{-3}$ in the gas phase and $180 \mu\text{g m}^{-3}$ in the particle phase. Other compounds were in the $0\text{--}10 \mu\text{g m}^{-3}$ range for the gas phase and the $0\text{--}35 \mu\text{g m}^{-3}$ range for the particle phase. The aerosol yield after all 13BD was consumed was 0.027 for an SOA concentration of $86 \mu\text{g m}^{-3}$. This yield is very similar to 0.025 measured by Sato et al. (2008). Figure 6 shows SOA yield as a function of the fraction of 13BD reacted. The aerosol yield started to increase when approximately 30% of 13BD was reacted and increased rapidly at approximately 95%. This growth curve can be divided in three regions (Figure 6). The first region is characteristic of no or very low aerosol formation. After ozone starts building up in the chamber (region II), more aerosol is formed as 13BD is reacted. After 13BD is completely reacted (region III), aerosol continues to increase, probably due to the oxidation of first and potentially second/third generation products resulting in a vertical section. Ng et al. (2006) reported a similar trend for compounds bearing two or more double bonds (isoprene, α -terpinene, γ -terpinene, terpinolene, limonene, myrcene, α -humulene, β -caryophyllene, and linalool).

3.3 Mechanism of product formation

Recent studies (Surratt et al., 2010; Sato et al., 2011; Lin et al., 2012, 2013; Pye et al., 2013; Birdsall et al., 2013, 2014) show the importance of epoxide chemistry in isoprene SOA formation. Methacrolein (MAC), methacryloylperoxynitrate (MPAN), and methacrylic acid epoxide (MAE) were proposed to be key intermediates in understanding mechanistic pathways leading to some isoprene reaction products either under low or high NO_x conditions. Of particular importance, species observed recently in isoprene-SOA including: 2-methylglyceric acid, 2-methyltetrols, 2-methylglyceric acid-oligomers, nitric acid esters, and sulfuric acid esters (Edney et al., 2005; Surratt et al., 2007; Szmigielski et al., 2007; Gomez-Gonzalez et al., 2008; Jaoui et al., 2008; Chan et al., 2010a, b; Nguyen et al., 2011; Hatch et al., 2011; Zhang et al., 2011). For example, MAE formed through MPAN chemistry (Surratt et al., 2010) was proposed to be key precursor to the formation of 2-methylglyceric acid and other oligoesters observed in isoprene

aerosol (Lin et al., 2013; Birdsall et al., 2013, 2014). Since isoprene and 1,3-butadiene only differ by one methyl group, it is likely they share similar gas and aerosol phase chemistries that yield SOA. 1,3-Butadiene presents a higher degree of symmetry than isoprene and may lead to a simpler set of mechanistic pathways. The detection in smog chamber experiments of similar end products from isoprene and 1,3-butadiene oxidation (e.g. methyltetrols vs tetrols, methylglyceric acid vs. glyceric acid, methacrolein vs. acrolein, methyl-oligoesters vs. oligoesters etc) suggests that the atmospheric oxidation of these two hydrocarbons may be similar.

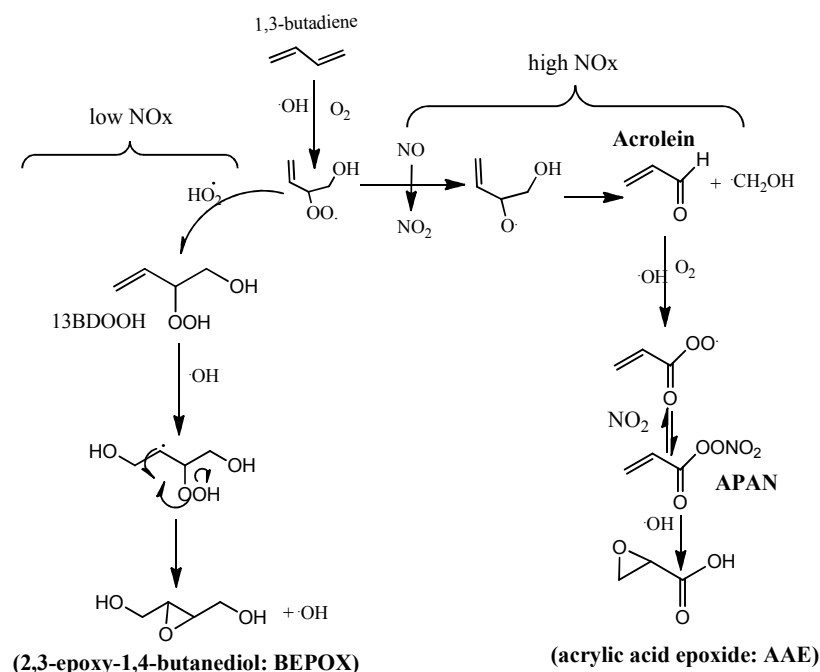
Time profiles from the static experiment (ER442: Table 1) involving 1,3-butadiene photooxidation in the presence of NO_x (Figures 4, 5) show an increase in the concentration of SOA compounds as ozone concentration increases. This indicates that ozone reaction is likely involved in the formation of SOA compounds, although under atmospheric conditions 1,3-butadiene oxidation with OH radicals is believed to be dominant. In the following discussion, tentative mechanistic pathways leading to some major products observed in the gas and particle phase are shown, based on either OH and/or ozone reactions. These mechanistic pathways are similar to those reported recently for isoprene. Acrolein, one of the major first generation product, was proposed to be formed through 1,3-butadiene reaction with OH radical, ozone, or O(³P) as shown in Scheme 1 (Liu et al., 1999). Other mechanistic pathways leading to some gas phase products



Scheme 1. Acrolein formation from 1,3-butadiene oxidation

observed in this study, including formaldehyde, glyoxal, glycolaldehyde, butenedial, malonaldehyde, have been reported (Liu et al., 1999) through either O₃ or OH reactions with 13BD and are not presented here.

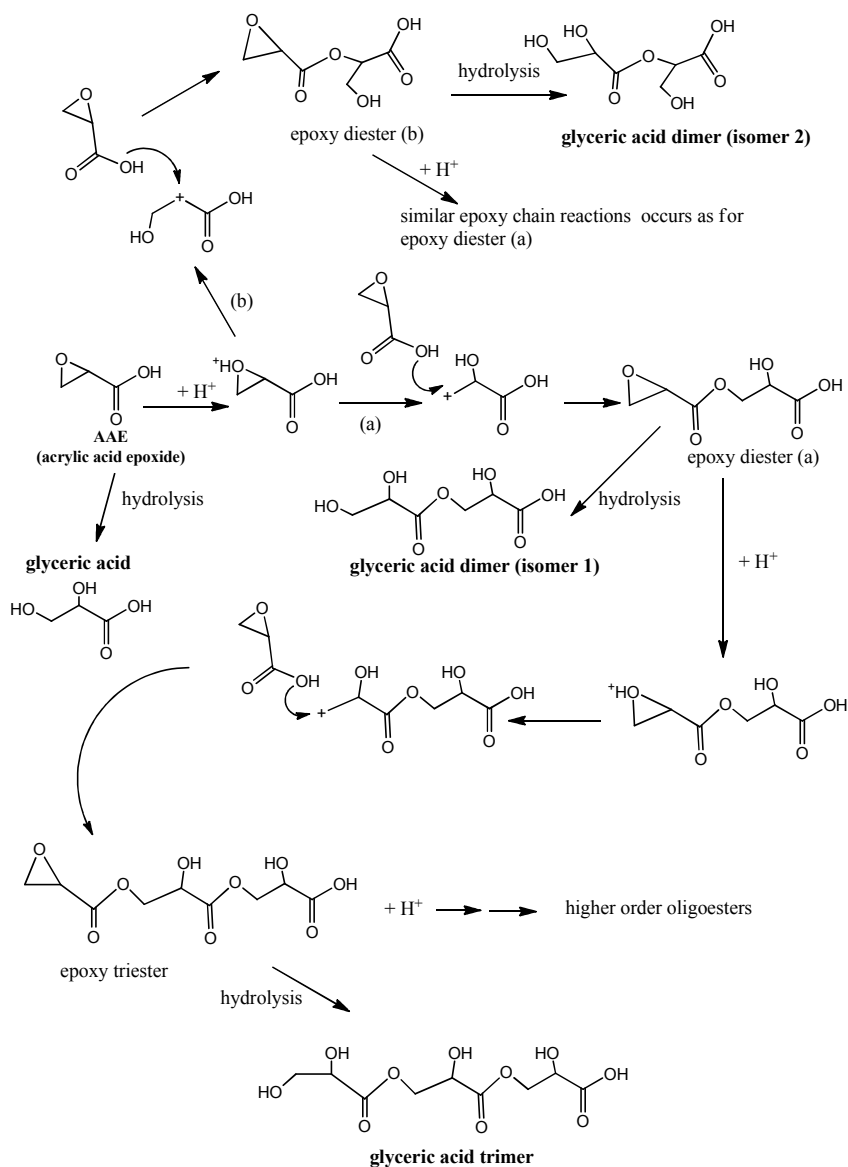
Recent studies show that epoxide species (e.g. IEPOX [low NO_x] and MAE [high NO_x] for isoprene) play an important role in understanding SOA formation (Paulot et al., 2009; Lin et al., 2013; Birdsall et al., 2014; Nguyen et al., 2014). Similar to isoprene chemistry, two epoxides (acrylic acid epoxide (AAE); and 2,3-epoxy-1,4-butanediol (BEPOX)) formed in the gas phase through the reaction of 13BD with OH radicals are proposed to be keys intermediates in SOA formation. Scheme 2 shows reaction pathways leading to the formation of acrylic acid epoxide (AAE: right side) and 2,3-epoxy-1,4-butanediol (BEPOX: left side) under high and low NO_x condition, respectively. These mechanistic pathways are similar to those proposed for isoprene (Paulot et al., 2009; Surratt et al., 2010; Lin et al., 2013; Nguyen et al., 2014; Birdsall et al., 2014) for the formation of MAE and IEPOX, respectively. Under low NO_x conditions, BEPOX is proposed to be formed through OH radical addition to one of the external positions of the double bonds to form hydroxyhydroperoxide (13BDOOH). Subsequent addition of OH radicals to the other double bond of 13BDOOH yields dihydroxyepoxide (BEPOX) as shown in left side (Scheme 2). In addition, 1,4-anhydroerythritol compound was detected in 1,3-BD SOA (Table 2). This compound is similar to 3-methyldihydroxytetrahydrofurans formed from the oxidation of isoprene through IEPOX oxidation via acid-catalyzed rearrangement on sulfate aerosol (Zhang et al., 2011; Lin et al., 2012). 1,4-Anhydroerythritol observed here may be formed through similar reactions starting from BEPOX, and presents further evidence that BEPOX is being formed from the oxidation of 1,3-BD and playing a role in SOA formation. In the presence of NO_x, Scheme 2 (right side) shows the formation of acrolein through 13BD reaction with OH radicals yielding hydroxyperoxy radicals, then acrolein (see also Scheme 1). Acrolein reacts with OH radicals, and in the presence of NO, yields the formation of APAN (Scheme 2: right side). Similar to MPAN (Lin et al., 2013), APAN is proposed to react with OH radicals leading to AAE compound.



Scheme 2. Proposed mechanism for AAE and BEPOX formation from 1,3-butadiene oxidation

Mass spectra obtained from GC-MS analysis of SOA originated from experiments involving NOx show the presence of a series of monomeric compounds as well as oligoesters structurally related to these monomers (Table 2). Although important advances has been made recently for isoprene chemistry to understand key intermediates species (epoxides) leading to SOA formation (Birdsall et al., 2014), the conditions necessary for their formation (e.g. acidity, water content, inorganic ions, etc) and the specific chemical mechanisms by which these compounds are formed remain unknown. Lin et al. (2013) and Birdsall et al. (2014) show the importance of MAE in the formation of methylglyceric acid as well as a wide range of oligoesters structurally related to 2-methylglyceric acid. For oligoesters formation, Birdsall et al. (2014) presented data suggesting that acid catalyzed nucleophilic addition of MAE is kinetically feasible in the atmosphere mainly under acidic conditions but much slower than the epoxide chain reaction. In addition, Birdsall et al. (2014) show that a series of nucleophile reactions may occurs in the atmosphere including self-reaction of MAE as well as MAE reaction with other nucleophilic compounds (water, acids, and alcohols). In this study, a series of oligoesters were observed and their formation may follow similar mechanistic pathways as those proposed by Birdsall et al. (2014) for isoprene reaction. Scheme 3 shows a proposed mechanism for AAE

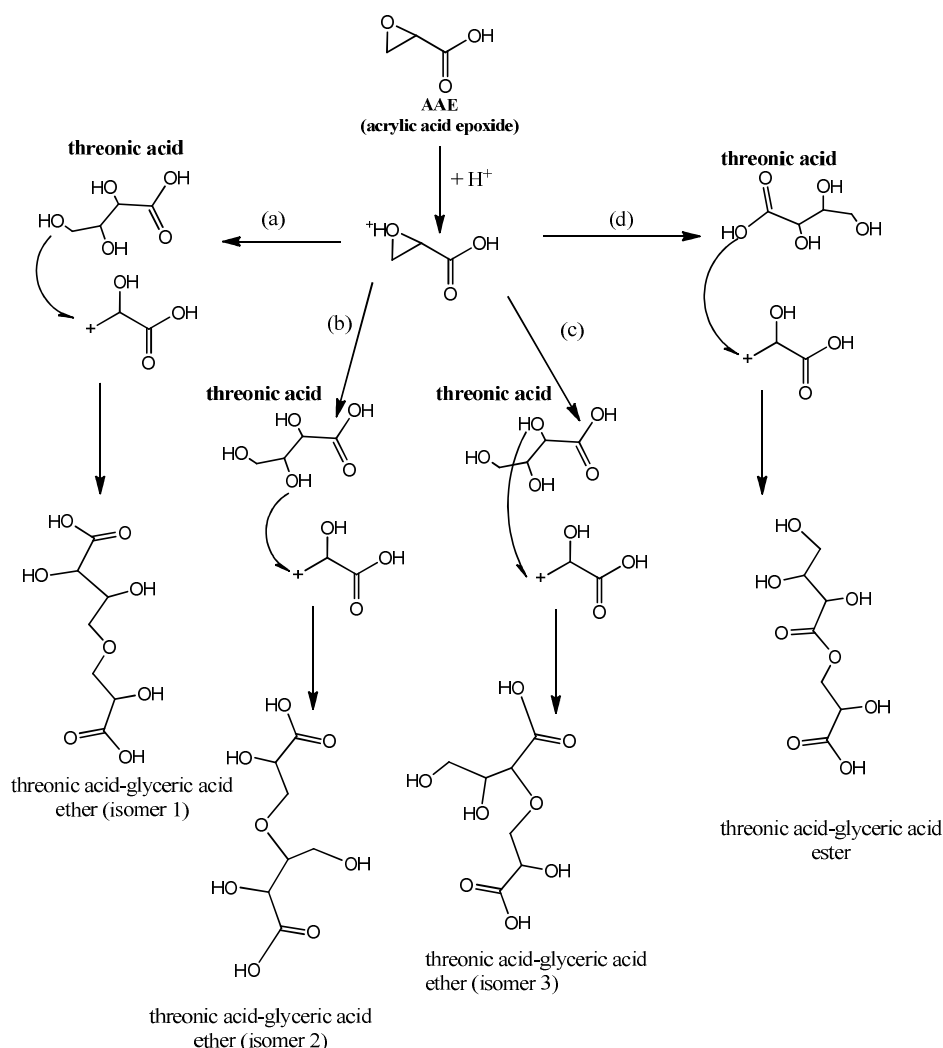
oligomerization via epoxy chain reaction. In the presence of H^+ , AAE undergoes nucleophilic addition leading to series of epoxy glyceric acid oligomers. Two pathways (a, b) are shown in Scheme 3 showing the formation of two isomers (e.g. glyceric acid dimer 1, and glyceric acid dimer 2). Each epoxy compounds may undergo hydrolysis leading to the corresponding monomer or oligomers.



Scheme 3. Proposed mechanism for AAE oligomerization via epoxy chain reaction leading to glyceric acid, and glyceric acid oligoesters

The detection in the aerosol phase of a series of oligoesters with structure characteristics of a combination of an alcohol and an acid compound (Table 2), suggests that reactions in the

aerosol phase between monomer compounds bearing alcohol and acid groups may occur. Recent work by Birdsall et al. (2013) show that classical esterification reactions involving reaction of organic acid and alcohol under atmospheric conditions is too slow to occur and cannot accounts for all the oligoesters observed in chamber experiments. Based on his work and prior work (Surratt et al., 2010; Lin et al., 2013), Birdsall et al. (2014) provided evidence that nucleophilic reaction between MAE and a series of nucleophilic compounds yields a series of oligoesters including ethers, esters, and diols. By analogy to MAE, we proposed in this study similar nucleophilic reactions between AAE and a series of nucleophilic products observed in this study



Scheme 4. Proposed mechanism for AAE + threonic acid via nucleophilic addition reaction

leading to ethers (3 isomers) and one ester (Table 2) (e.g. acids (oxalic acid, malic acid, threonic acid); alcohols (tetrols, glycerol etc)). As an example, Scheme 4 shows proposed mechanism of

AAE and threonic acid reaction via nucleophilic addition. The nucleophilic addition of threonic acid, a trihydroxy acid, to AAE involves all three alcoholic OH groups leading to the formation of three ethers compounds (pathways a, b, and c), as well as the carboxylic COOH group leading to the formation of an ester (pathway d).

None of these oligoesters were detected in ambient samples analyzed using the same derivatization techniques suggesting that oligoesters may be formed mainly under laboratory conditions where high concentration of AAE and other nucleophile species are present. In addition, under atmospheric condition, water and other non-epoxide nucleophile compounds may limit the formation of oligoesters due to competitive hydrolysis pathway when epoxides are formed (Scheme 3). This is consistent with the work reported by Birdsall et al. (2014) involving MAE nucleophilic reactions.

3.4 Field measurements

Some organic compounds observed in the gas phase in laboratory samples are also present in ambient air. High concentrations of formaldehyde, glyoxal, acrolein, and APAN were observed from 13BD oxidation. Data reported in the literature show that these compounds are ubiquitous in urban ambient samples and suggest that 13BD might be a contributing source of these compounds in areas dominated by 13BD emission rates. In addition, the uptake of some of these compounds (e.g., glyoxal) in the aerosol phase followed by heterogeneous sulfur chemistry can lead to SOA formation (Carlton et al., 2007; Liggitto et al., 2005, Chan et al., 2010). The role of APAN in ambient SOA formation could be important and might follow similar chemistry as methacryloylperoxynitrate (MPAN), which only recently was found to play a role in SOA formation from isoprene (Tanimoto and Akimoto, 2001; Surratt et al., 2010).

Of great interest are eighth organic compounds observed in both laboratory and field sample particle phase. These compounds are shown in Figure 7 in an extracted ion chromatogram of a PM_{2.5} sample collected in Bakersfield, CA (Liu et al., 2012). A comparison of mass spectra from the laboratory sample with those measured at the field site is shown in Figure 8 for glyceric acid, *D*-threitol, erythrose, and threonic acid. Glycerol, glyceric acid, malic acid, threitol, erythritol, and tartaric acid were previously observed in ambient sample and have been thought to have originated from several sources, although their origin is still associated with high

uncertainty. From this work, it now appears that these compounds could be generated in the atmosphere from the oxidation of 13BD. Additionally glyceric acid, threitol, erythritol, erythrose, and threonic acid observed in this study appear to have originated only from 13BD. An analysis of chromatograms obtained from chamber experiments conducted in our laboratory involving the oxidation of biogenic (e.g., isoprene, monoterpenes, sesquiterpenes, 2-methyl-3-buten-2-ol), aromatic (e.g., toluene, 1,3,5-trimethylbenzene, benzene), and polycyclic aromatic hydrocarbons (PAHs) (e.g., naphthalene) shows that these compounds were not detected in these systems using the same experimental analysis. In fact, in selected ambient samples, particularly those collected in an urban environment, glyceric acid, threitol, erythritol, erythrose, and threonic acid have been detected in this study. Although the nine compounds were detected in several field samples analyzed by our group (e.g., Cleveland Multiple Air Pollutant Study [CMAPS] field study, Piletic et al., 2013; Midwestern United States, Lewandowski et al., 2007, 2008), the field samples analyzed for this paper focus on 27 samples collected in Bakersfield, CA between May 19, 2010 and June 26, 2010. The concentrations of malic acid, glyceric acid, erythritol, erythrose, and threonic acid (*d*-threonic acid + *meso*-threonic acid) were determined in ambient samples using the same method used for static experiment ER442. The total PM_{2.5} mass in the atmosphere during this sampling period ranged from 0.06 to 1.17 ug m⁻³. The concentrations for individual compounds ranged from 0 and 14.1 ng m⁻³. These values are typical of the range of values often seen for individual compounds detected in ambient samples.

3.5. Summary

In the present manuscript, laboratory experiments were conducted to investigate SOA formation from the oxidation of 1,3-butadiene in the presence and absence of NO_x. Chamber aerosol collected under these conditions have been analyzed for organic mass to organic carbon ratio, effective enthalpy of vaporization, and aerosol yield. In addition, the chemical composition of the gas phase and SOA was analyzed using derivative-based methods followed by gas chromatography–mass spectrometry or high-performance liquid chromatography analysis of the derivative compounds. More than 60 oxygenated organic compounds in the gas and particle phases were observed, of which 31 organic monomers were tentatively identified. The major products identified are glyceric acid, *d*-threitol, erythritol, *d*-threonic acid, *meso*-threonic acid,

erythrose, malic acid, tartaric acid, and carbonyls including glycolaldehyde, glyoxal, acrolein, malonaldehyde, glyceraldehyde, and peroxyacryloyl nitrate (APAN).

Two epoxides compounds, BEPOX and AAE, are proposed in this study to be key intermediates for the formation of an important class of 13BD-derived compounds including glyceric acid and oligoesters found in SOA. Similar to isoprene oxidation (Birdsall et al., 2014), the mechanism proposed is based on epoxide chain reaction of AAE, as well as AAE reaction with a number of nucleophile species including water, carboxylic acids and alcohols. The BEPOX channel is also an important pathway leading to ambient SOA formation. However, none of these oligoesters were detected in ambient samples, suggesting that oligoesters may be formed mainly under laboratory conditions where high concentration of AAE and other nucleophile species are present. These oligoesters under ambient conditions may be not stable and after their decomposition could be possible sources of glyceric acid, threonic acid and tetrols found in ambient aerosol.

The results of this study potentially have atmospheric implications for areas impacted by 1,3-butadiene oxidation and contribute to understanding the formation of ambient SOA from small anthropogenic precursors. For instance, several compounds were detected and identified in both field and smog chamber SOA (e.g. malic acid, glyceric acid, erythritol, erythrose, and threonic acid) and suggest that they might be responsible for the formation and/or the growth of the aerosol in region impacted by 13BD emission. The presence of nucleophile compounds (acids, alcohols, epoxides) and aldehyde including dicarbonyls (e.g. glyoxal), and their potential for heterogeneous and multiphase processes is also very interesting. However, in the absence of authentic standards, it is difficult to accurately quantify the contribution of SOA originating from 13BD to ambient PM_{2.5}. Due to the health risks associated with 13BD and its reaction products, this work indicates the importance of increasing the inclusion of detailed chemistry of 13BD into photochemical models and local, regional and global models used to investigate ozone and SOA formation and health concerns to rural and urban areas.

Disclaimer. The U.S. Environmental Protection Agency through its Office of Research and Development funded and collaborated in the research described here under Contract EP-D-10-070 to Alion Science and Technology. The manuscript has been subjected to external peer review and has been cleared for publication. Mention of trade names or commercial products does not constitute endorsement or recommendation for use.

References

- 2 Acquavella, J. F.: Butadiene epidemiology: a summary of results and outstanding issues,
Toxicology, 113, 148–156, 1996.
- 4 Angove, D. E., Fookes, C. J. R., Hynes, R.G., Walters, C. K., and Azzi, M.: The
characterisation of secondary organic aerosol formed during the photodecomposition of 1,3-
6 butadiene in air containing nitric oxide, Atmos. Environ., 40, 4597–4607, 2006.
- 8 Anttinen-Klemetti, T., Vaaranrinta, R., Mutanen, P., and Peltonen, K.: Inhalation exposure
to 1,3-butadiene and styrene in styrene-butadiene copolymer production, Int. J. Hyg. Environ.
Health, 209, 151–158, 2006.
- 10 Atkinson, R.: Atmospheric chemistry of VOCs and NO_x, Atmos. Environ., 2063–2101,
2000.
- 12 Berndt, T., and Böge, O.: Atmospheric reaction of OH radicals with 1,3-butadiene and 4-
hydroxy-2-butenal, J. Phys. Chem. A, 111, 12099–12105, 2007.
- 14 Birdsall, A. W., Zentner, C. A., and Elrod, M. J.: Study of the kinetics and equilibria of
the oligomerization reactions of 2-methylglyceric acid, Atmos. Chem. Phys., 13, 3097–3109,
16 doi:10.5194/acp-13-3097-2013, 2013.
- 18 Birdsall, A. W., Miner, C. R., Mael, L. E., and Elrod, M. J.: Mechanistic study of
secondary organic aerosol components formed from nucleophilic addition reactions of
methacrylic acid epoxide, Atmos. Chem. Phys. Discuss., 14, 19917–19954, 2014.
- 20 Carlton, A. G., Turpin, B. J., Altieri, K. E., Seitzinger, S., Reff, A., Lim, H.-J., and
Ervens, B.: Atmospheric oxalic acid and SOA production from glyoxal: results of aqueous
22 photooxidation experiments, Atmos. Environ., 41, 7588–7602, 2007.
- 24 Chan, A.W. H., Chan, M. N., Surratt, J. D., Chhabra, P. S., Loza, C. L., Crounse, J. D.,
Yee, L. D., Flagan, R. C., Wennberg, P. O., and Seinfeld, J. H.: Role of aldehyde chemistry and
NO_x concentrations in secondary organic aerosol formation, Atmos. Chem. Phys., 10, 7169–
26 7188, 25 doi:10.5194/acp-10-7169-2010, 2010a.
- 28 Chan, M. N., Surratt, J. D., Claeys, M., Edgerton, E. S., Tanner, R. L., Shaw, S. L.,
Zheng, M., Knipping, E. M., Eddingsaas, N. C., Wennberg, P. O., and Seinfeld, J. H.:

Characterization and quantification of isoprene-derived epoxydiols in ambient aerosol in the
southeastern United States, *Environ. Sci. Technol.*, 44, 4590–4596, 2010b.

Charlson, R. J., Schwartz, S. E., Hales, J. M., Cess, R. D., Coakley Jr., J. A., Hansen, J.
E., and Hoffman, D. J.: Climate forcing by anthropogenic aerosols, *Science*, 255, 423–430,
doi:10.1126/science.255.5043.423, 1992.

Claeys, M., Graham, B., Vas, G., Wang, W., Vermeylen, R., Pashynska, V., Cafmeyer, J.,
Guyon, P., Andreae, M. O., Artaxo, P., and Maenhaut W.: Formation of secondary organic
aerosols through photooxidation of isoprene, *Science*, 303, 1173–1176, 2004.

Claeys, M., Kourtchev, I., Pashynska, V., Vas, G., Vermeylen, R., Wang, W., Cafmeyer,
J., Chi, X., Artaxo, P., Andreae, M. O., and Maenhaut, W.: Polar organic marker compounds in
atmospheric aerosols during the LBA-SMOCC 2002 biomass burning experiment in Rondônia,
Brazil: sources and source processes, time series, diel variations and size distributions, *Atmos.
Chem. Phys.*, 10, 9319–9331, 2010.

Decesari, S., Fuzzi, S., Facchini, M. C., Mircea, M., Emblico, L., Cavalli, F., Maenhaut,
W., Chi, X., Schkolnik, G., Falkovich, A., Rudich, Y., Claeys, M., Pashynska, V., Vas, G.,
Kourtchev, I., Vermeylen, R., Hoffer, A., Andreae, M. O., Tagliavini, E., Moretti, F., and Artaxo,
P.: Characterization of the organic composition of aerosols from Rondônia, Brazil, during the
LBA-SMOCC 2002 experiment and its representation through model compounds, *Atmos. Chem.
Phys.*, 6, 375–402, 2006.

Dollard, G. J., Dore, C. J., and Jenkin, M. E.: Ambient concentrations of 1,3-butadiene in
the UK, *Chem. Biol. Interact.*, 135, 177–206, 2001.

Duffy, B. L., and Nelson, P. F.: Exposure to emissions of 1,3-butadiene and benzene in
the cabins of moving motor vehicles and buses in Sydney, Australia, *Atmos. Environ.*, 31, 3877–
3885, 1997.

Doyle, M., Sexton, K. G., Jeffries, H., Bridge, K., and Jaspers, I.: Effects of 1,3-butadiene,
isoprene, and their photochemical degradation products on human lung cells, *Environ Health
Perspect.* 112(15), 1488–1495, 2004.

Eatough, D. J., Hansen, L. D., and Lewis, E. A.: The chemical characterization of
environmental tobacco smoke, *Environ. Technol.*, 11, 1071–1085, 1990.

Edney, E. O., Kleindienst, T. E., Jaoui, M., Lewandowski, M., Offenberg, J. H., Wang,
2 W., and Claeys M.: Formation of 2-methyl tetrols and 2-methylglyceric acid in secondary organic
aerosol from laboratory irradiated isoprene/NO_x/SO₂/air mixtures and their detection in ambient
4 PM_{2.5} samples collected in the eastern United States, *Atmos. Environ.*, 39, 5281–5289, 2005.

Ekström, S., Nozière, B., and Hansson, H.-C.: The cloud condensation nuclei (CCN)
6 properties of 2-methyltetrols and C3-C6 polyols from osmolality and surface tension
measurements, *Atmos. Chem. Phys.*, 9, 973–980, 2009.

Fu, P. Q., Kawamura, K., Pavuluri, C. M., Swaminathan, T., and Chen, J.: Molecular
8 characterization of urban organic aerosol in tropical India: contributions of primary emissions and
secondary photooxidation, *Atmos. Chem. Phys.*, 10, 2663–2689, 2010.

Gómez-González, Y., Surratt, J. D., Cuyckens, F., Szmigielski, R., Vermeylen, R., Jaoui,
12 M., Lewandowski, M., Offenberg, J. H., Kleindienst, T. E., Edney, E. O., Blockhuys, F., Van
Alsenoy, C., Maenhaut, W., and Claeys, M.: Characterization of organosulfates from the
14 photooxidation of isoprene and unsaturated fatty acids in ambient aerosol using liquid
chromatography/(-) electrospray ionization mass spectrometry, *J. Mass Spectrom.*, 43, 371–382,
16 doi:10.1002/jms.1329, 2008.

Grosjean, D., and Seinfeld, J. H.: Parameterization of the formation potential of secondary
18 organic aerosols, *Atmos. Environ.*, 23, 1733–1747, 1989.

Hallquist, M., Wenger, J. C., Baltensperger, U., Rudich, Y., Simpson, D., Claeys, M.,
20 Dommen, J., Donahue, N. M., George, C., Goldstein, A. H., Hamilton, J. F., Herrmann, H.,
Hofmann, T., Iinuma, Y., Jang, M., Jenkin, M. E., Jimenez, J. L., Kiendler-Scharr, A., Maenhaut,
22 W., McFiggans, G., Mentel, Th. F., Monod, A., Prev'ot, A. S. H., Seinfeld, J. H., Surratt, J. D., ^
Szmigielski, R., and Wildt, J.: The formation, properties and impact of secondary organic aerosol:
24 current and emerging issues, *Atmos. Chem. Phys.*, 9, 5155–5236, doi:10.5194/acp-9-
5155-2009, 2009.

Hatch, L. E., Creamean, J. M., Ault, A. P., Surratt, J. D., Chan, M. N., Seinfeld, J. H.,
26 Edgerton, E. S., Su, Y., and Prather, K. A.: Measurements of isoprene-derived organosul10 fates
in ambient aerosols by aerosol time-of-flight mass spectrometry – Part 1: Single particle
28 atmospheric observations in Atlanta, *Environ. Sci. Technol.*, 45, 5105–5111,
30 doi:10.1021/es103944a, 2011a.

- Hatch, L. E., Creamean, J. M., Ault, A. P., Surratt, J. D., Chan, M. N., Seinfeld, J. H.,
2 Edgerton, E. S., Su, Y., and Prather, K. A.: Measurements of isoprene-derived organosulfates in
ambient aerosols by aerosol time-of-flight mass spectrometry – Part 2: Temporal variability and
4 formation mechanisms, *Environ. Sci. Technol.*, 45, 8648–8655, doi:10.1021/es2011836, 2011b.
- Hurst, H. E.: Toxicology of 1,3-butadiene, chloroprene, and isoprene, *Rev. Environ.*
6 *Contam. Toxicol.*, 189, 131–179, 2007.
- Jaoui, M., Kleindienst, T. E., Lewandowski, M., and Edney, E. O.: Identification and
8 quantification of aerosol polar oxygenated compounds bearing carboxylic or hydroxyl groups. 1.
Method development, *Anal. Chem.*, 76, 4765–4778, 2004.
- 10 Jaoui, M., Kleindienst, T. E., Lewandowski, M., Offenberg, J. H., and Edney E. O.:
Identification and quantification of aerosol polar oxygenated compounds bearing carboxylic or
12 hydroxyl groups. 2. Organic tracer compounds from monoterpenes, *Environ. Sci. Technol.*, 39,
5661–5673, 2005.
- 14 Jaoui, M., Edney, E. O., Kleindienst, T. E., Lewandowski, M., Offenberg, J. H., Surratt, J.
D., and Seinfeld, J. H.: Formation of secondary organic aerosol from irradiated α -
16 pinene/toluene/NO_x mixtures and the effect of isoprene and sulfur dioxide, *J. Geophys. Res.*, 113,
D09303 doi:10.1029/2007jd009426, 2008.
- 18 Jaoui, M., Kleindienst, T. E., Offenberg, J. H., Lewandowski, M., and Lonneman, W. A.:
SOA formation from the atmospheric oxidation of 2-methyl-3-buten-2-ol and its implications for
20 PM_{2.5}, *Atmos. Chem. Phys.*, 12, 2173–2188, doi:10.5194/acp-12-2173-2012, 2012.
- Kanakidou, M., Seinfeld, J. H., Pandis, S. N., Barnes, I., Dentener, F. J., Facchini, M. C.,
22 Van Dingenen, R., Ervens, B., Nenes, A., Nielsen, C. J., Swietlicki, E., Putaud, J. P., Balkanski,
Y., Fuzzi, S., Horth, J., Moortgat, G. K., Winterhalter, R., Myhre, C. E. L., Tsigaridis, K.,
24 Vignati, E., Stephanou, E. G., and Wilson, J.: Organic aerosol and global climate modelling: a
review, *Atmos. Chem. Phys.*, 5, 1053–1123, 2005.
- 26 Kleindienst, T. E., Edney, E. O., Lewandowski, M., Offenberg, J. H. and Jaoui M.:
Secondary organic carbon and aerosol yields from the irradiations of isoprene and alpha-pinene in
28 the presence of NO_x and SO₂. *Environ. Sci. Technol.*, 40, 3807–3812, 2006.

Kleindienst, T. E., Jaoui, M., Lewandowski, M., Offenberg, J. H., Lewis, C. W., Bhave, P. V., and Edney, E. O.: Estimates of the contributions of biogenic and anthropogenic hydrocarbons to secondary organic aerosol at a southeastern US location, *Atmos. Environ.*, 41, 8288–8300, 2007.

Kleindienst, T. E., Lewandowski, M., Offenberg, J. H., Jaoui, M., and Edney, E. O.: The formation of secondary organic aerosol from the isoprene + OH reaction in the absence of NO_x, *Atmos. Chem. Phys.*, 9, 6541–6558, 2009.

Kleindienst, T. E., Lewandowski, M., Offenberg, J. H., Edney, E. O., Jaoui, M., Zheng, M., Ding, X., and Edgerton, E. S.: Contribution of primary and secondary sources to organic aerosol and PM_{2.5} at SEARCH network sites, *J. Air Waste Manag. Assoc.*, 60, 1388–1399, 2010.

Kroll, J. H., Ng, N. L., Murphy, S. M., Flagan, R. C., and Seinfeld, J. H.: Secondary organic aerosol formation from isoprene photooxidation, *Environ. Sci. Technol.*, 40, 1869–1877, 2006.

Kramp, F., and Paulson, S. E.: The gas phase reaction of ozone with 1,3-butadiene: formation yields of some toxic products, *Atmos. Environ.*, 34, 35–43, 2000.

Lewandowski, M., Jaoui, M., Kleindienst, T. E., Offenberg, J. H., and Edney, E. O.: Composition of PM_{2.5} during the summer of 2003 in Research Triangle Park, North Carolina, *Atmos. Environ.*, 41, 4073–4083, 2007.

Lewandowski, M., Jaoui, M., Offenberg, J. H., Kleindienst, T. E., Edney, E. O., Sheesley, R. J., and Schauer, J. J.: Primary and secondary contributions to ambient PM in the midwestern United States, *Environ. Sci. Technol.*, 42, 3303–3309, 2008.

Lewandowski, M., Jaoui, Offenberg, J. O., Krug, J., and Kleindienst, T. E.: Atmospheric oxidation of 1, 3-butadiene: 2. influence of aerosol acidity and relative humidity, Submitted to *Atmos. Chem. Phys. Discuss.*

Liggio, J., Li, S.-M., and McLaren, R.: Reactive uptake of glyoxal by particulate matter, *J. Geophys. Res. Atmos.*, 110, D10304, doi:10.1029/2004JD005113, 2005.

Lin, Y.-H., Zhang, Z., Docherty, K. S., Zhang, H., Budisulistiorini, S. H., Rubitschun, C. L., Shaw, S. L., Knipping, E. M., Edgerton, E. S., Kleindienst, T. E., Gold, A., and Surratt, J. D.:

Isoprene epoxydiols as precursors to secondary organic aerosol formation: Acid-catalyzed

reactive uptake studies with authentic compounds, *Environ. Sci. Technol.*, 46, 250–258, 2012.

Lin, Y.-H., Zhang, H., Pye, H. O. T., Zhang, Z., Marth, W. J., Park, S., Arashiro, M., Cui, T., Budisulistiorini, S. H., Sexton, K. G., Vizuete, W., Xie, Y., Luecken, D. J., Piletic, I. R., Edney, E. O., Bartolotti, L. J., Gold, A., and Surratt, J. D.: Epoxide as a precursor to secondary organic aerosol formation from isoprene photooxidation in the presence of nitrogen oxides, *P. Natl. Acad. Sci. USA*, 110, 6718–6723, doi:10.1073/pnas.1221150110, 2013.

Liu, S., Ahlm, L., Day, D. A., Russell, L. M., Zhao, Y., Gentner, D. R., Weber, R. J., Goldstein, A. H., Jaoui, M., Offenberg, J. H., Kleindienst, T. E., Rubitschun, C., Surratt, J. D., Sheesley, R. J., and Scheller, S.: Secondary organic aerosol formation from fossil fuel sources contribute majority of summertime organic mass at Bakersfield. *J. Geophys. Res. Atmos.*, 117, doi:10.1029/2012JD018170, 2012.

Liu, X., Jeffries, H. E., and Sexton, K. G.: Hydroxyl radical and ozone initiated photochemical reactions of 1,3-butadiene, *Atmos. Environ.*, 33, 3005–3022, 1999.

Ng, N. L., Kroll, J. H., Keywood, M. D., Bahreini, R. A., Varutbangkul, V., Flagan, R. C., Seinfeld, J. H.: Contribution of First- versus Second-Generation Products to Secondary Organic Aerosols Formed in the Oxidation of Biogenic Hydrocarbons, *Environ. Sci. Technol.*, 40, 2283–2297, 2006.

Nguyen, T. B., Roach, P. J., Laskin, J., Laskin, A., and Nizkorodov, S. A.: Effect of humidity on the composition of isoprene photooxidation secondary organic aerosol, *Atmos. Chem. Phys.*, 11, 6931–6944, doi:10.5194/acp-11-6931-2011, 2011.

Nguyen, T. B., Coggon, M. M., Bates, K. H., Zhang, X., Schwantes, R. H., Schilling, K. A., Loza, C. L., Flagan, R. C., Wennberg, P. O., and Seinfeld, J. H.: Organic aerosol formation from the reactive uptake of isoprene epoxydiols (IEPOX) onto non-acidified inorganic seeds, *Atmos. Chem. Phys.*, 14, 3497–3510, 2014.

Notario, A., Le Bras, G., and Mellouki, A.: Kinetics of Cl atom reactions with butadienes including isoprene, *Chem. Phys. Lett.*, 281, 421–425, 1997.

Offenberg, J. H., Kleindienst, T. E., Jaoui, M., Lewandowski, M., and Edney, E.O.: Thermal properties of secondary organic aerosols, *Geophys. Res. Lett.*, 33, L03816, doi:10.1029/2005GL024623, 2006.

Pankow, J. F., Luo, W., Tavakoli, A. D., Chen, C., and Isabelle, L. M.: Delivery levels and behavior of 1,3-butadiene, acrylonitrile, benzene, and other toxic volatile organic compounds in mainstream tobacco smoke from two brands of commercial cigarettes, *Chem. Res. Toxicol.*, 17, 805–813, 2004.

Paulot, F., Crounse, J. D., Kjaergaard, H. G., Kürten, A., St. Clair, J. A., Seinfeld, J. H., and Wennberg, P. O.: Unexpected epoxide formation in the gas-phase photooxidation of isoprene, *Science*, 325, 730–732, 2009.

Penn, A., and Snyder, C. A.: 1,3-butadiene, a vapor phase component of environmental tobacco smoke, accelerates arteriosclerotic plaque development, *Circulation*, 93, 552–557, 1996.

Piletic, I. R., Offenberg, J. H., Olson, D. A., Jaoui, M., Krug, J., Lewandowski, M., Turlington, J. M., and Kleindienst, T. E: Constraining carbonaceous aerosol sources in a receptor model by including ^{14}C data with redox species, organic tracers, and elemental/organic carbon measurements, *Atmos. Environ.*, 80, 216–225, 2013.

Pope III, C. A., Ezzati, M., and Dockery, D. W.: Fine-particulate air pollution and life expectancy in the United States, *N. Engl. J. Med.*, 360, 376–386, doi: 10.1056/NEJMsa0805646, 2009.

Pye, H. O. T., Pinder, R.W., Piletic, I. R., Xie, Y., Capps, S. L., Lin, Y.-H., Surratt, J. D., Zhang, Z., Gold, A., Luecken, D. J., Hutzell, W. T., Jaoui, M., Offenberg, J. H., Kleindienst, T. E., Lewandowski, M., and Edney, E. O.: Epoxide pathways improve model predictions of isoprene markers and reveal key role of acidity in aerosol formation, *Environ. Sci. Technol.*, 47, 11056–11064, doi:10.1021/es402106h, 2013.

Sato, K.: Detection of nitrooxypolyols in secondary organic aerosol formed from the photooxidation of conjugated dienes under high- NO_x conditions, *Atmos. Environ.*, 42, 6851–6861, 2008.

Sato, K., Nakao, S., Clark, C. H., Qi, L., and Cocker III, D. R.: Secondary organic aerosol formation from the photooxidation of isoprene, 1,3-butadiene, and 2,3-dimethyl-1,3-butadiene under high NO_x conditions, *Atmos. Chem. Phys.*, 11, 7301–7317, 2011.

Sisler, J. F., and Malm, W. C.: The relative importance of soluble aerosols to spatial and seasonal trends of impaired visibility in the United States, *Atmos. Environ.*, 28, 851–862, 1994.

- Smith, D. F., Kleindienst, T. E., and Hudgens, E. E.: Improved high-performance liquid chromatographic method for artifact-free measurements of aldehydes in the presence of ozone using 2,4-dinitrophenylhydrazine, *J. Chromatogr. A*, 483, 431–436, 1989.
- Sorsa, M., Peltonen, K., Anderson, D., Demopoulos, N. A., Neumann, H. G., and Osterman-Golkar, S.: Assessment of environmental and occupational exposures to butadiene as a model for risk estimation of petrochemical emissions, *Mutagenesis*, 11, 9–17, 1996.
- Surratt, J. D., Murphy, S. M., Kroll, J. H., Ng, N. L., Hildebrandt, L., Sorooshian, A., Szmigielski, R., Vermeylen, R., Maenhaut, W., Claeys, M., Flagan, R. C., and Seinfeld, J. H.: Chemical composition of secondary organic aerosol formed from the photooxidation of isoprene, *J. Phys. Chem. A*, 110, 9665–9690, 2006.
- Surratt, J. D., Lewandowski, M., Offenberg, J. H., Jaoui, M., Kleindienst, T. E., Edney, E. O., and Seinfeld, J. H.: Effect of acidity on secondary organic aerosol formation from isoprene, *Environ. Sci. Technol.*, 41, 5363–5369, 2007.
- Surratt, J. D., Chan, A. W. H., Eddingsaas, N. C., Chan, M., Loza, C. L., Kwan, A. J., Hersey, S. P., Flagan, R. C., Wennberg, P. O., and Seinfeld, J. H.: Reactive intermediates revealed in secondary organic aerosol formation from isoprene, *Proc. Natl. Acad. Sci. USA*, 107, 6640–6645, 2010.
- Szmigielski, R., Surratt, J. D., Vermeylen, R., Szmigielska, K., Kroll, J. H., Ng, N. L., Murphy, S. M., Sorooshian, A., Seinfeld, J. H., and Claeys, M.: Characterization of 2-methylglyceric acid oligomers in secondary organic aerosol formed from the photooxidation of isoprene using trimethylsilylation and gas chromatography/ion trap mass spectrometry, *J. Mass. Spectrom.*, 42, 101–116, 2007.
- Tanimoto, H., and Akimoto, H.: A new peroxydicarboxylic nitric anhydride identified in the atmosphere: $\text{CH}_2=\text{CHC}(\text{O})\text{OONO}_2$ (APAN), *Geophys. Res. Lett.*, 28, 2831–2834, 2001.
- Thornton-Manning, J. R., Dahl, A. R., Bechtold, W. E., Griffith Jr, W. C., and Henderson, R. F.: Comparison of the disposition of butadiene epoxides in Sprague-Dawley rats and B6C3F1 mice following a single and repeated exposures to 1,3-butadiene via inhalation, *Toxicology*, 123, 125–134, 1997.

United States Environmental Protection Agency (US EPA), Locating and estimating air emissions from sources of 1,3-butadiene, EPA-454/R-96-008, Office of Air Quality Planning and Standards: Research Triangle Park, NC, 1996.

United States Environmental Protection Agency (US EPA), Health Assessment of 1,3-butadiene, EPA/600/P-98/001F, Office of Research and Development: Washington, DC, 2002.

Vimal, D., Pacheco, A. B., Iyengar, S. S., and Stevens, P. S.: Experimental and ab initio dynamical investigations of the kinetics and intramolecular energy transfer mechanisms for the OH + 1,3-butadiene reaction between 263 and 423 K at low pressure, *J. Phys. Chem. A*, 112, 7227–7237, 2008.

Wang, W., Wu, M. H., Li, L., Zhang, T., Liu, X. D., Feng, J. L., Li, H. J., Wang, Y. J., Sheng, G. Y., Claeys, M., and Fu, J. M.: Polar organic tracers in PM_{2.5} aerosols from forests in eastern China, *Atmos. Chem. Phys.*, 8, 7507–7518, 2008.

Zhang, H., Surratt, J. D., Lin, Y-H., Bapat, J., and Kamens, R. M.: Effect of relative humidity on SOA formation from isoprene/NO photooxidation: enhancement of 2-methylglyceric acid and its corresponding oligoesters under dry conditions. *Atmos. Chem. Phys.* 11(13): 6411–6424, 2011.

Zhang, Z., Lin, Y. H., Zhang, H., Surratt, J. D., Ball, L. M., and Gold, A.: Technical note: Synthesis of isoprene atmospheric oxidation products: Isomeric epoxydiols and the rearrangement products cis- and trans-3-methyl-3,4-dihydroxytetrahydrofuran, *Atmos. Chem. Phys.*, 12, 8529–8535, doi:10.5194/acp-12-8529 2012, 2012.

Zhang, H., Zhang, Z., Cui, T., Lin, Y-H., Bhathela, N. A., Ortega, J., Worton, D. R., Goldstein, A. H., Guenther, A., Jimenez, J. L., Gold, A., and Surratt, J. D.: Secondary organic aerosol formation via 2-methyl-3-buten-2-ol photooxidation: evidence of acid-catalyzed reactive uptake of epoxides, *Environ. Sci. Technol. Lett.*, 1 (4), pp 242–247, 2014.

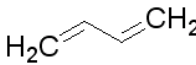
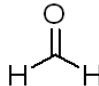
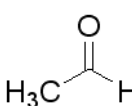
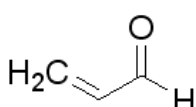
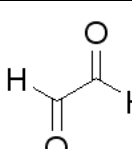
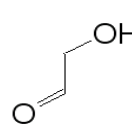
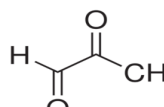
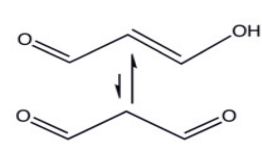
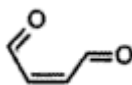
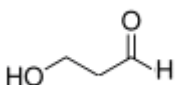
Ye, Y., Galbally, I. E., Weeks, I. A., Duffy, B. L., and Nelson, P. F.: Evaporative emissions of 1,3-butadiene from petrol-fuelled motor vehicles, *Atmos. Environ.*, 32, 2685–2692, 1998.

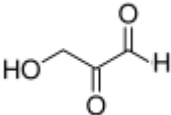
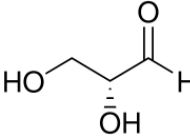
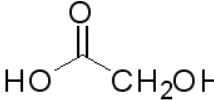
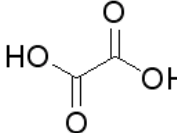
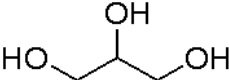
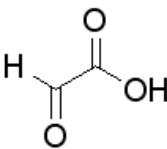
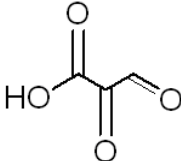
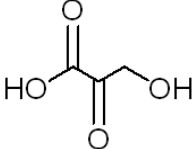
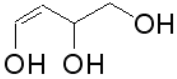
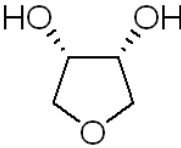
Table 1. Initial conditions for experiments involving 1,3-butadiene (13BD) oxidation. The experiments were conducted with the chamber operated in a dynamic (flow mode) except for ER439 and ER442 conducted in static (batch-mode). T: temperature; RH: relative humidity. Seed aerosol at 10 ug/m³ was used. GC-MS analysis was done only when NO_x was present in the system.

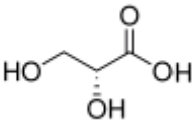
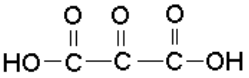
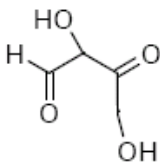
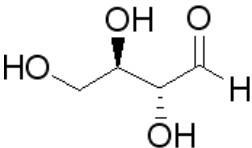
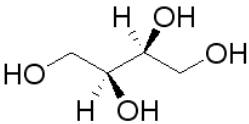
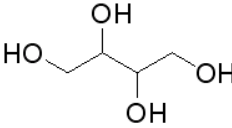
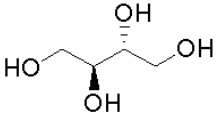
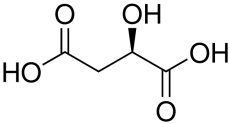
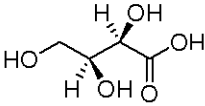
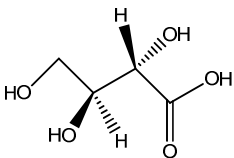
Exp. No.	Purpose	13BD (ppmC)	13BD (μg m ⁻³)	NO (ppb)	H ₂ O ₂ (ppm)	T (°C)	RH (%)
ER439	Test, compounds identification	8.4	4614	553	-	-	< 3
ER440-1	Tracers, parameters	6.3	3454	917	-	22	< 3
ER440-2	Tracers, parameters	3.2	1736	917	-	22	< 3
ER441-1	Tracers	5.4	2973	-	2.2	24	< 3
ER442	Time series, tracers	5.8	3186	724	-	-	< 3
ER443-1	Tracers	6.3	3487	-	3.8	24	< 3
ER444-1	Tracers, parameters	6.7	3656	340	-	22	30

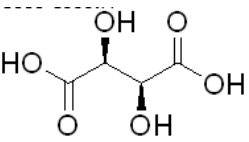
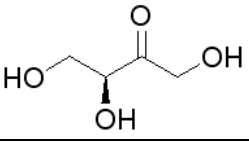
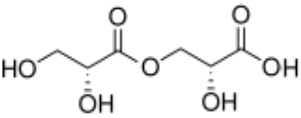
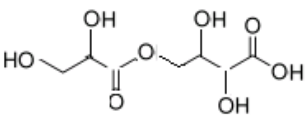
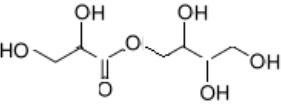
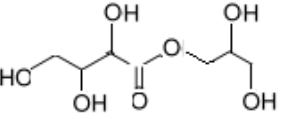
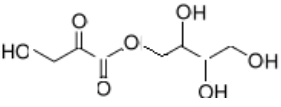
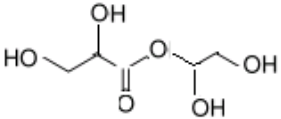
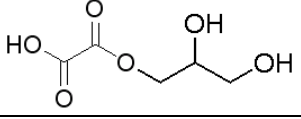
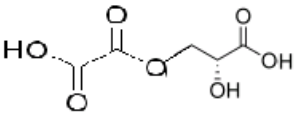
6

Table 2. Summary of gas-phase and SOA products generated from the oxidation of 1,3-butadiene. Oligoesters presented here are only one possible isomer.

Nomenclature	Structure	MW (g mol ⁻¹)	BSTFA MW (g mol ⁻¹)
1,3-Butadiene		54	-
Gas phase			
Formaldehyde		30	-
Acetaldehyde		44	-
Acrolein		56	-
Glyoxal		58	-
Glycolaldehyde		60	-
Methylglyoxal		72	-
Malonaldehyde		72	-
Butenedial		74	-
3-Hydroxy-propanaldehyde		74	-

Hydroxypyruvaldehyde		88	-
Glyceraldehyde		90	-
Particle phase			
Glycolic acid		76	220
Oxalic acid		90	234
Glycerol		92	308
Glyoxylic acid		74	146
Oxopyruvic acid		102	174
Hydroxypyruvic acid		104	248
1,3,4-Trihydroxy-1-butene		104	320
1,4-Anhydroerythritol		104	248

Glyceric acid		106	322
Ketomalonic acid		118	262
2,4-Dihydroxy-1,3-butanedione		118	262
Erythrose		120	336
L-Threitol		122	410
DL-Threitol		122	410
<i>meso</i> -Erythritol		122	410
Malic acid		134	350
Threonic acid		136	424
Erythreonic acid		136	424

L-Tartaric acid		150	438
Erythrulose		120	336
Oligoesters: particle phase			
Glyceric acid dimer		194	482
Glyceric acid-threonic acid ester		224	584
Glyceric acid-threitol ester		210	570
Threonic acid-glycerol ester		210	570
Hydroxypyruvic acid-tetrol ester		208	496
Glyceric acid-glycerol ester		180	468
Oxalic acid-glycerol ester		164	380
Oxalic acid-MW104	-	176	392
Oxalic acid-glyceric acid		178	394

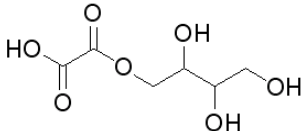
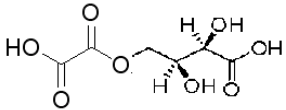
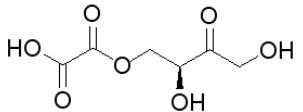
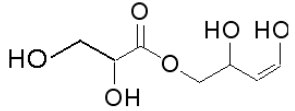
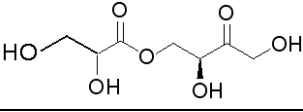
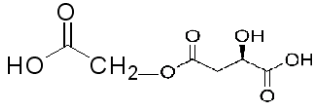
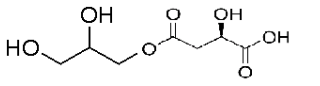
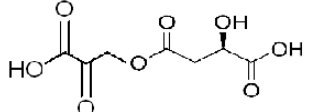
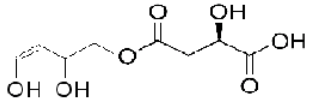
Oxalic acid-tetrol		190	478
Oxalic acid-threonic acid ester		208	496
Oxalic acid-erythrulose ester		192	408
Glyceric acid-1,3,4-trihydroxy-1-butene ester		192	480
Glyceric acid- erythrulose ester		224	512
Malic acid-glycolic acid ester		192	408
Malic acid-glycerol		208	496
Malic acid-hydroxypyruvic acid ester		220	436
Malic acid-1,3,4-trihydroxy-1-butene ester		220	508

Table 3. Reacted 1,3-butadiene and steady-state parameters determined from SOA produced by

2 1,3-butadiene oxidation.

Experiment No.	Reacted HC ($\mu\text{g m}^{-3}$)	Reacted HC ($\mu\text{g C m}^{-3}$)	O ₃ (ppb)	SOA ($\mu\text{g m}^{-3}$)	SMPS (nl m^{-3})	SOC ($\mu\text{g C m}^{-3}$)
ER440-1	3412	3028	487	140.2	117.5	49.8
ER440-2	1731	1536	382	34.7	31.4	12.4
ER441-1	1558	1382	48	37.7	33.5	13.6
ER443-1	1434	1273	28	22.5	18.6	8.6
ER444-1	2724	2417	281	-	-	17.2

In ER 444-1 high aerosol seed concentration was used, and SOA parameters were not reported for this experiment.

4

Table 4. OM/OC ratio, SOA and SOC yields, $\Delta H_{\text{vap}}^{\text{eff}}$, and density determined from 1,3-

2 butadiene photooxidation from dynamic experiments.

Experiment No.	OM/OC	Y_{SOA}	Y_{SOC}	$\Delta H_{\text{vap}}^{\text{eff}}$ (kJ mol ⁻¹)	Density
ER440-1	2.8	0.041	0.016	-27.32	1.2
ER440-2	2.8	0.020	0.008	-27.28	1.1
ER441-1	2.8	0.024	0.010	-25.38	1.1
ER443-1	2.6	0.016	0.007	-24.37	1.2
ER444-1	-	-	0.007	-	-
Avg. \pm S.D.	2.7 ± 0.09	0.025 ± 0.011	0.017 ± 0.013	-26.08 ± 1.46	1.2 ± 0.05

In ER 444-1 high aerosol seed concentration was used, and SOA parameters were not reported for this experiment.

4

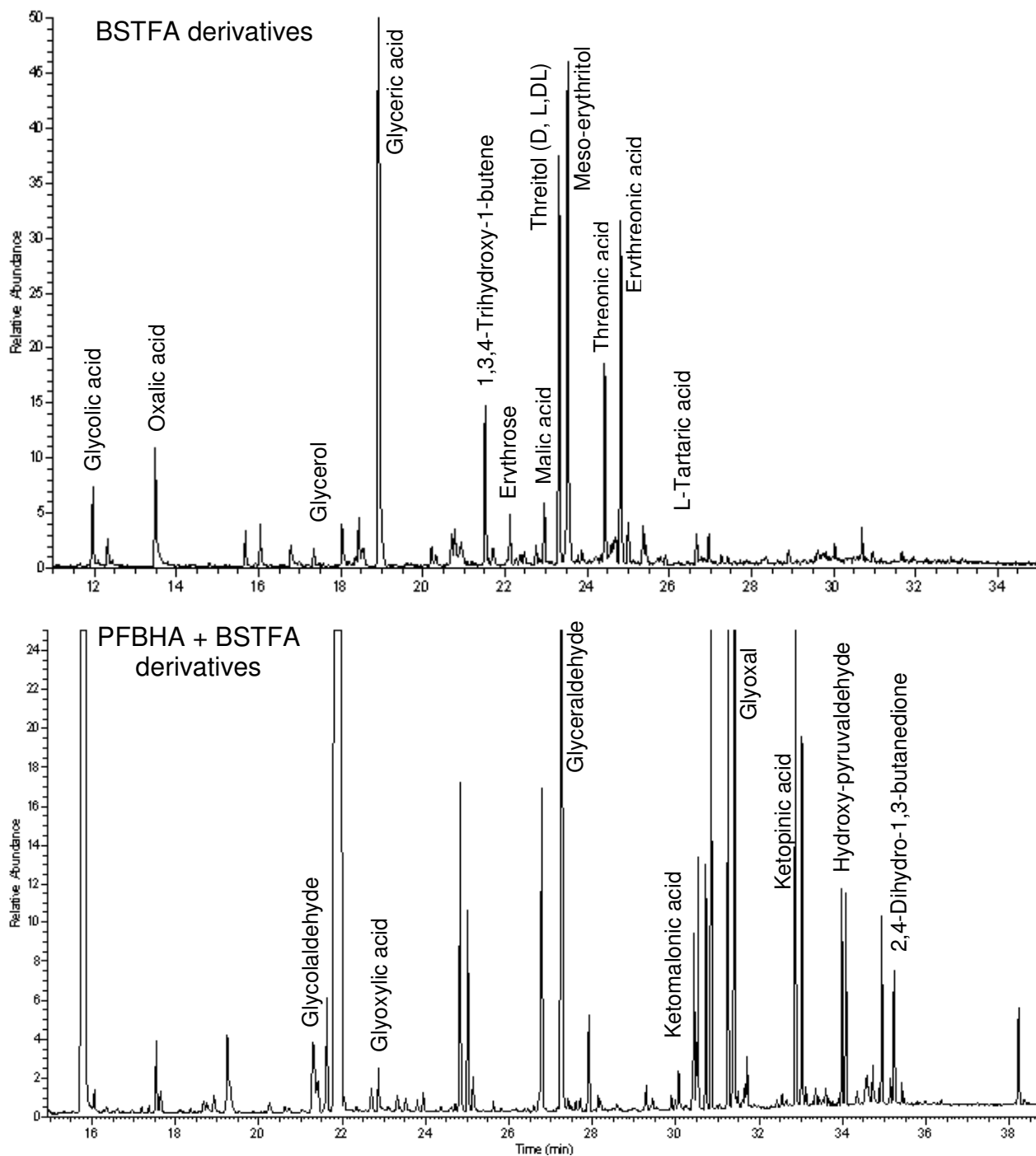


Figure 1. Total ion chromatograms of organic extracts from an irradiated 1,3-butadiene/NO_x/air mixture as BSTFA (top) and PFBHA + BSTFA (bottom) derivatives.

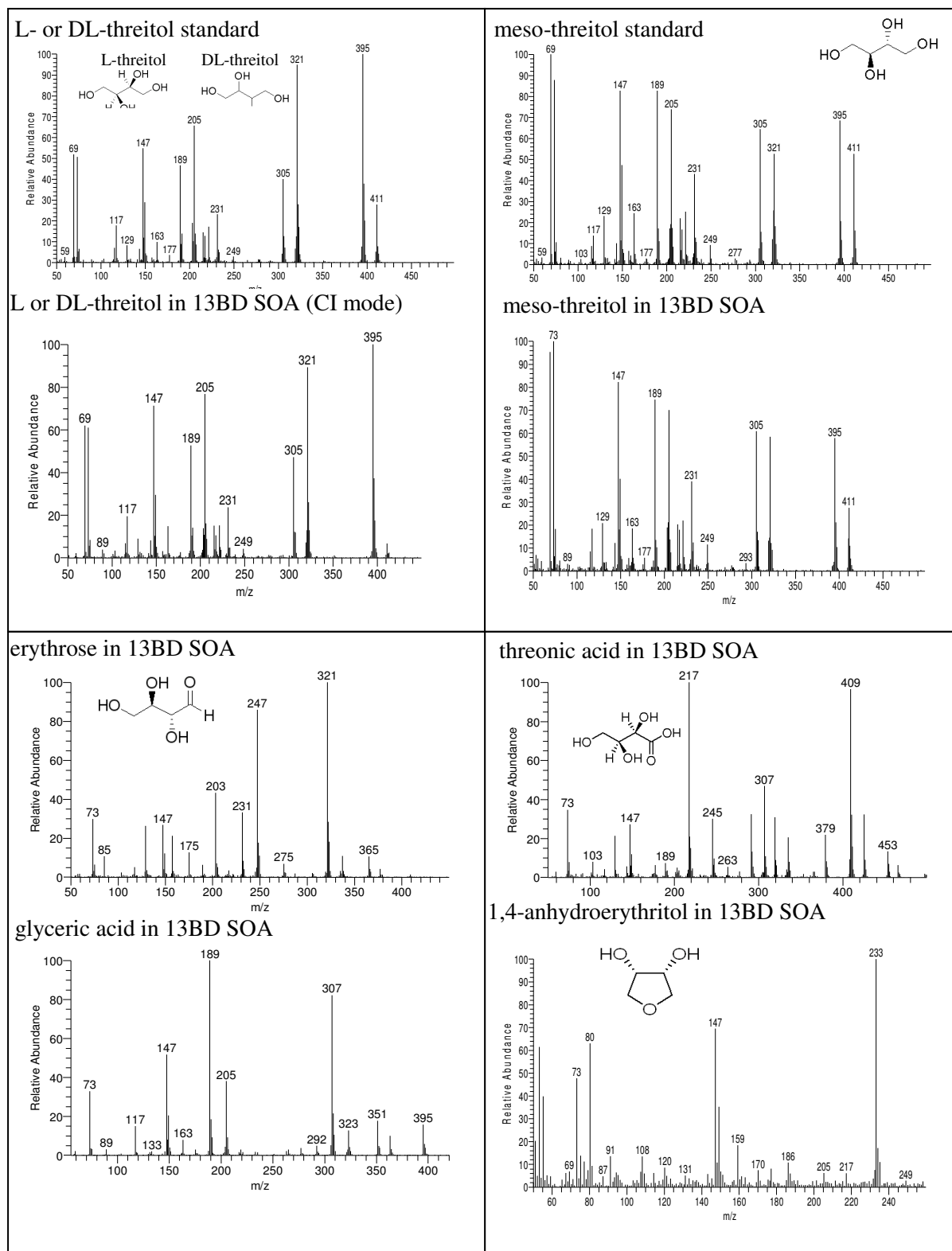
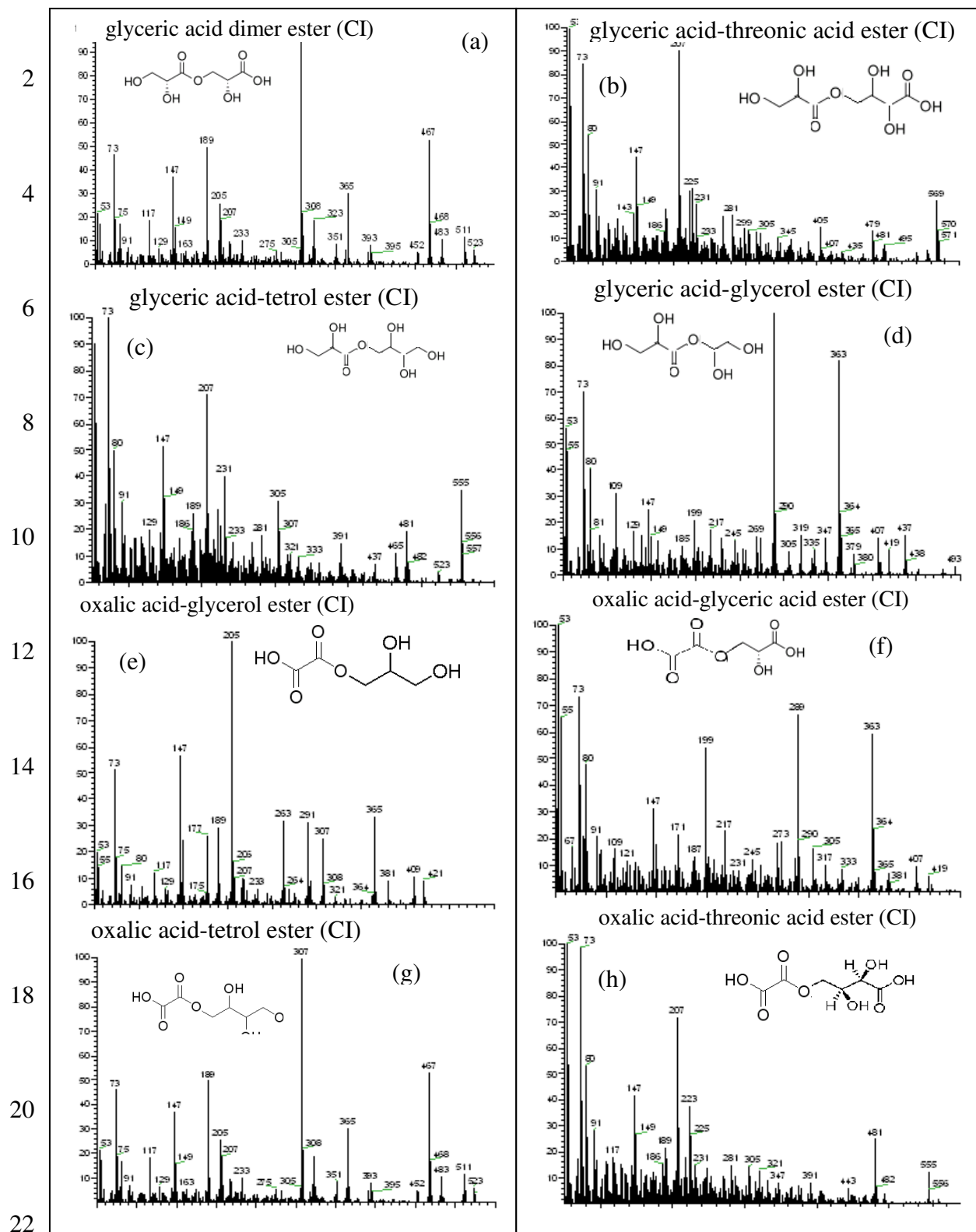
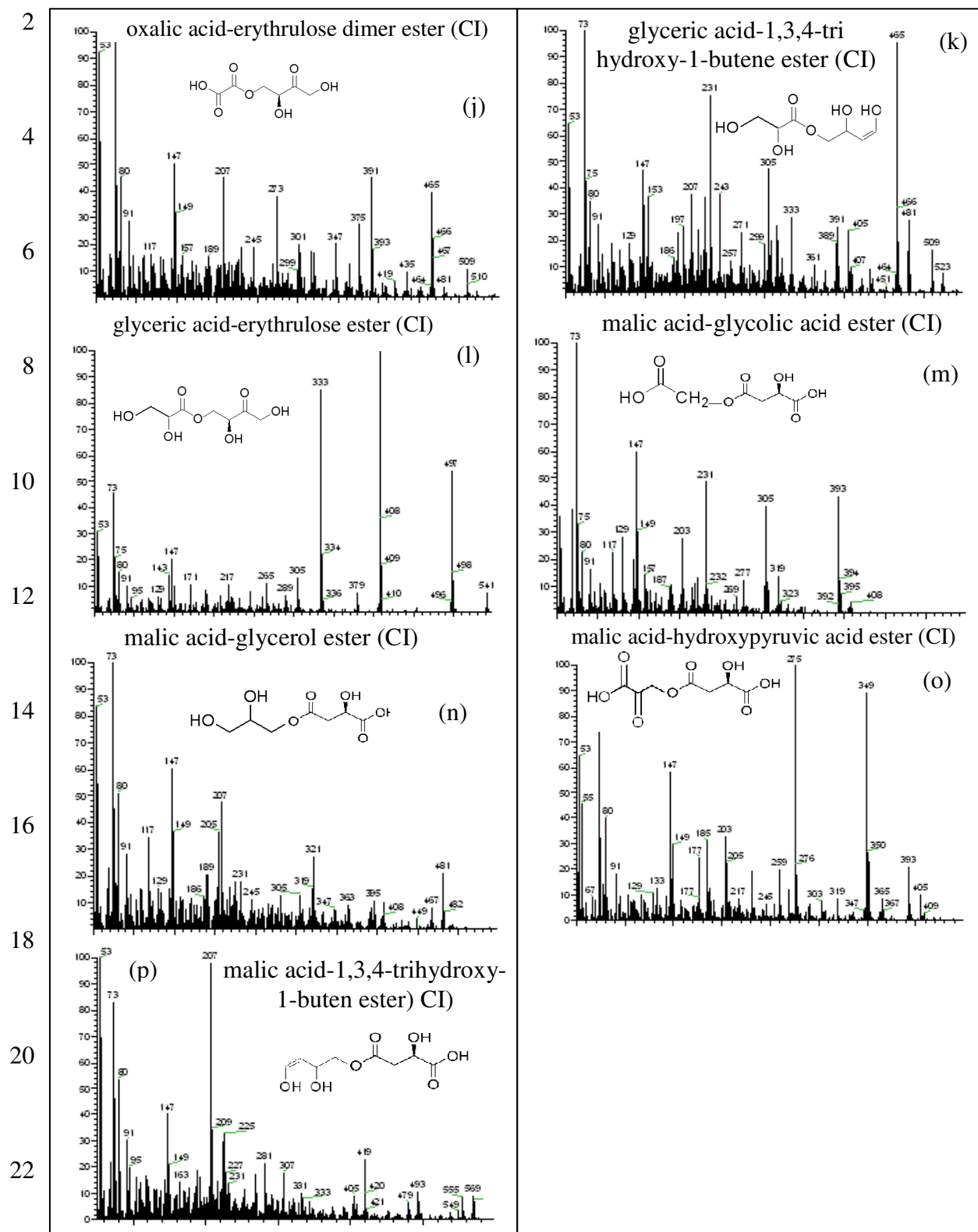


Figure 2. CI mass spectra of some organic compounds present in irradiated 1,3-butadiene/NO_x/air.





24 **Figure 3.** CI mass spectra of oligoester compounds present in irradiated 1,3-butadiene/NOx/air.

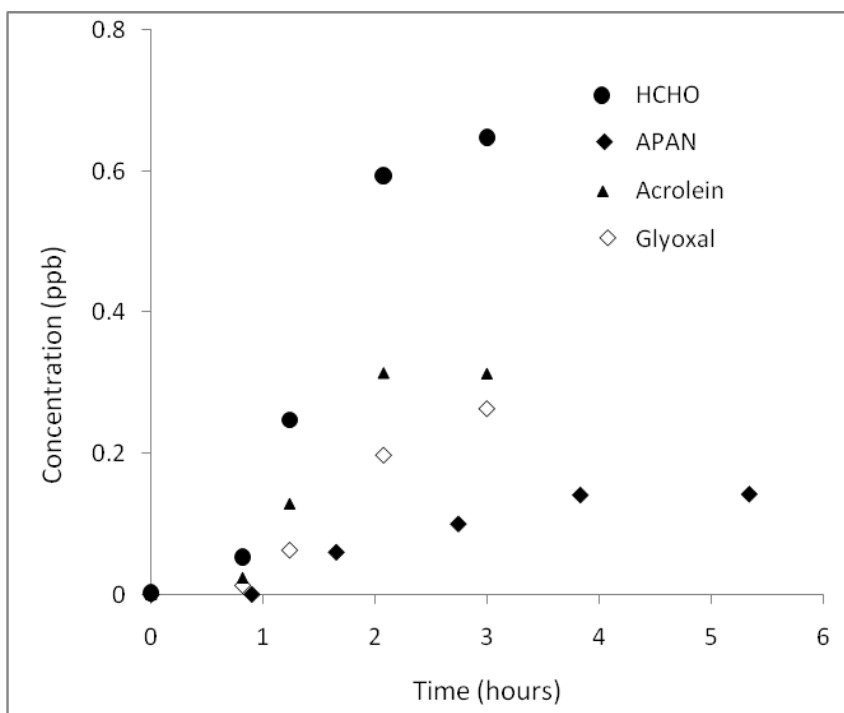
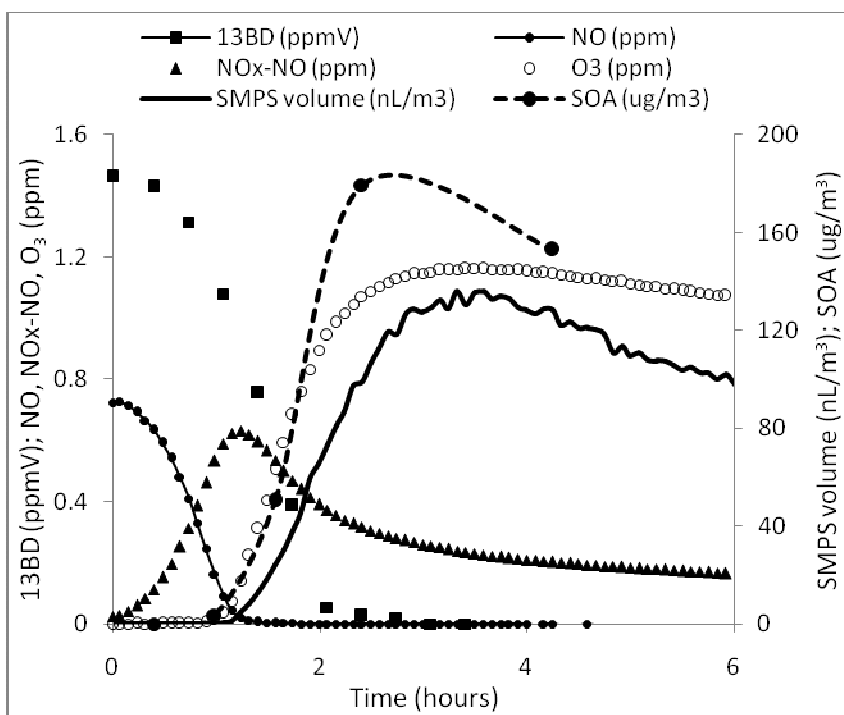
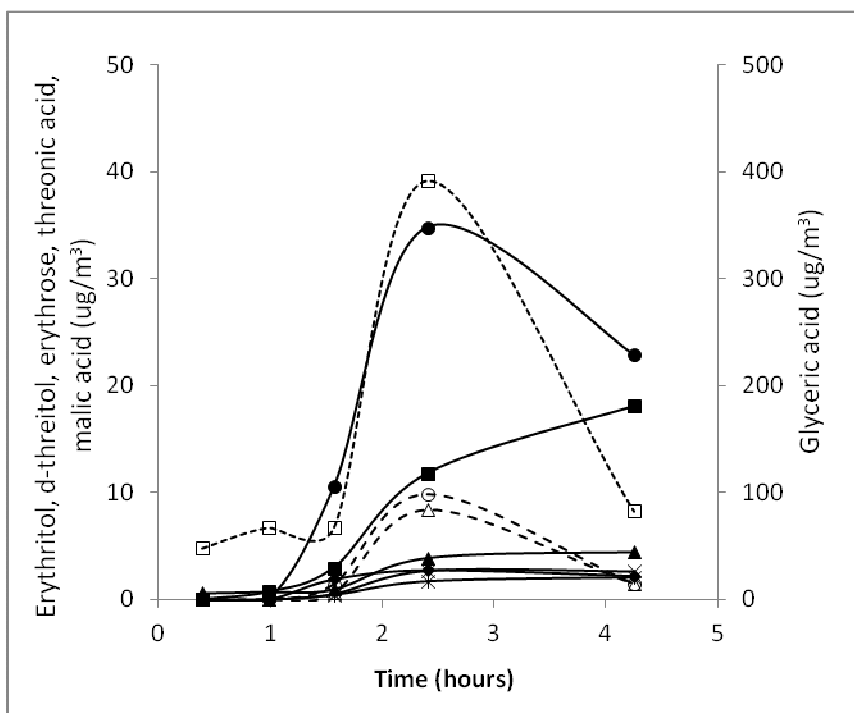
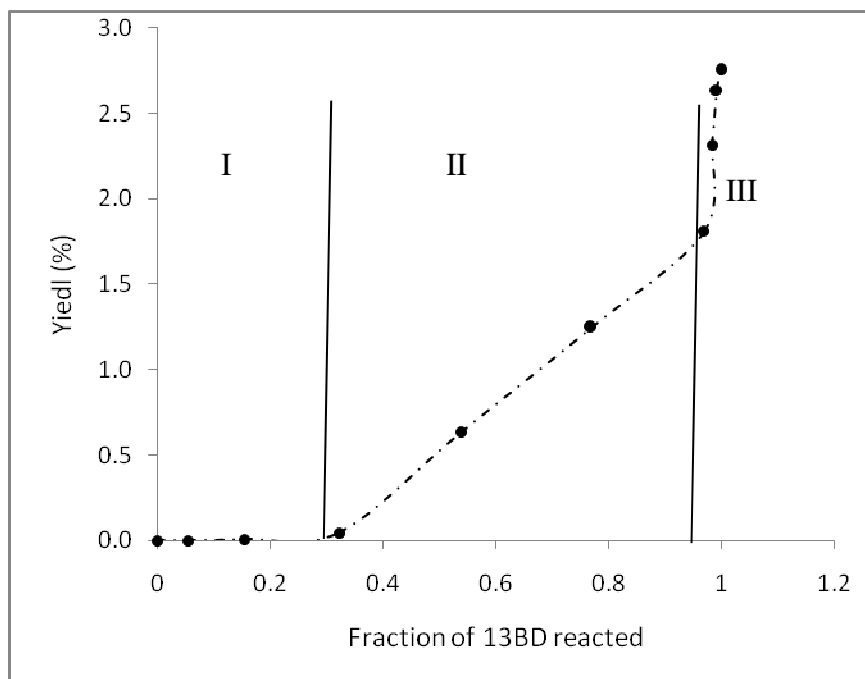


Figure 4. Time profile of gas-phase species from the oxidation of 13BD in experiment ER-442.

All species were corrected for dilution.



2 **Figure 5.** Time profile of gas- and particle-phase products from the oxidation of 13BD in
 experiment ER442. Quantitative analysis was done as BSTFA derivatives. d-Threitol was used as
 4 surrogate to quantify erythritol, threonic acid and malic acid. Particle phase/gas phase: (■)/(□) glyceric
 acid; (●)/(○) threonic acid; (▲)/(Δ) erythrose; (◆)/(◇) malic acid; (*)/(*/) threitol.



2

4 **Figure 6.** SOA yield as a function of the fraction of 13BD reacted (experiment ER442).

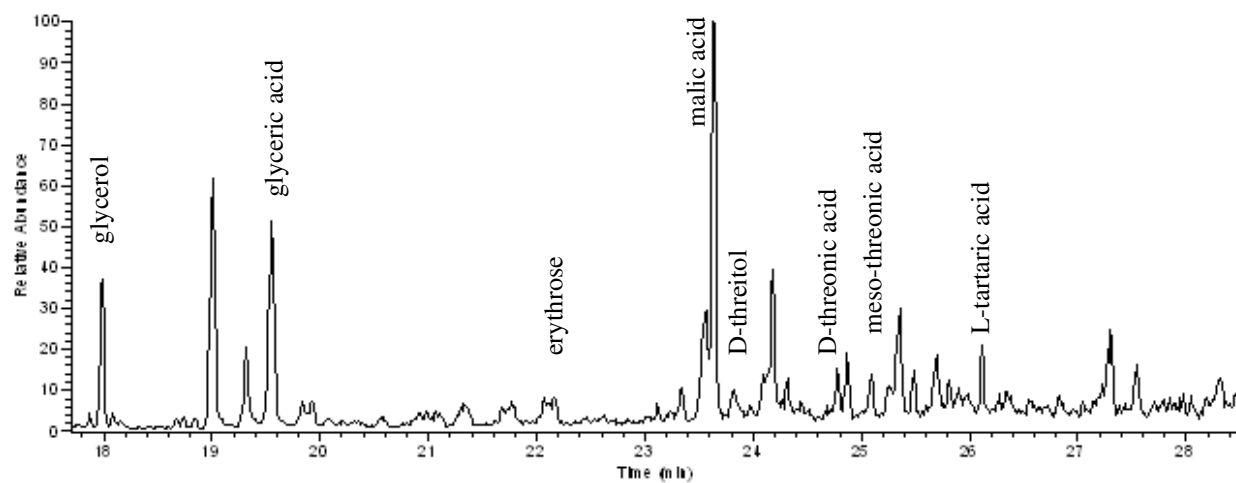
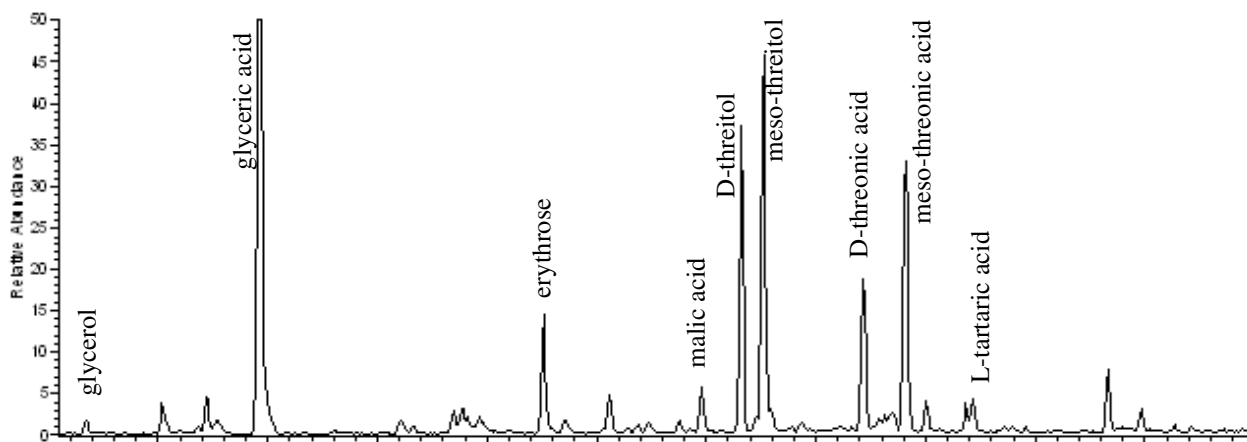


Figure 7. Extracted ion gas chromatograms of organic extracts as BSTFA derivatives from (top) an irradiated 1,3-butadiene/NO_x/air mixture and (bottom) Bakersfield western United States PM_{2.5}. Extracted ions are 103, 189, 217, 247, 335, 395, and 423.

2
4
6
8
10
12
14
16
18
20
22

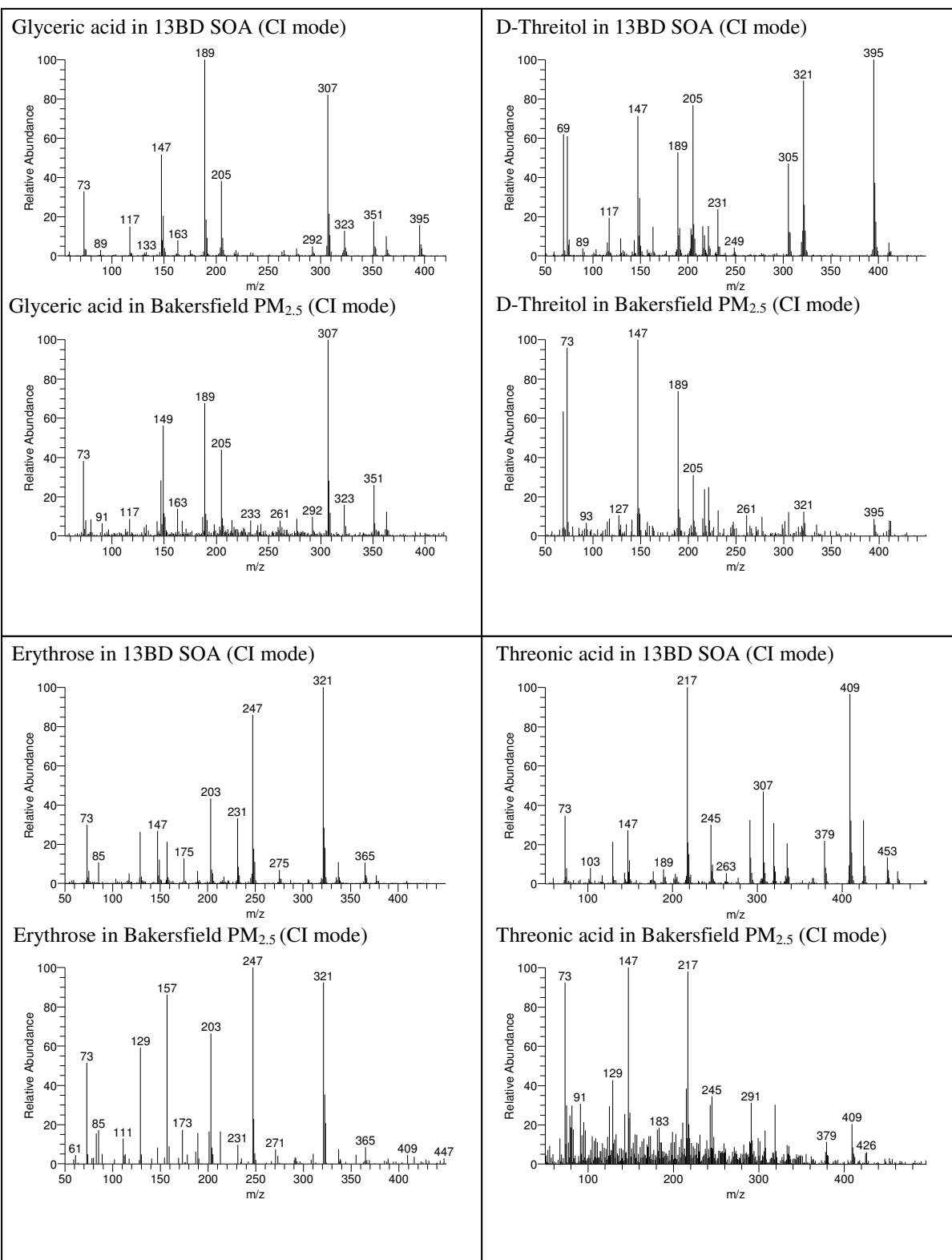


Figure 8. CI mass spectra of some organic compounds present in irradiated 1,3-butadiene/NO_x/air and in ambient PM_{2.5} extracts originated from field sample in the western US Bakersfield, CA.